Fixed-time synchronization of octonion-valued neural networks with mixed delays

A non-separation norm approach

Authors
Agrawal, Vaibhav; Singh, Sunny; Singh, Vineet Kumar; Das, Subir

DOI
10.1016/j.neucom.2025.130995

Publication date
2025

Document Version
Final published version

Published in
Neurocomputing

Citation (APA)
Agrawal, V., Singh, S., Singh, V. K., & Das, S. (2025). Fixed-time synchronization of octonion-valued neural networks with mixed delays: A non-separation norm approach. *Neurocomputing*, *652*, Article 130995. https://doi.org/10.1016/j.neucom.2025.130995

Neurocomputing 652 (2025) 130995

Contents lists available at ScienceDirect

Neurocomputing

journal homepage: www.elsevier.com/locate/neucom

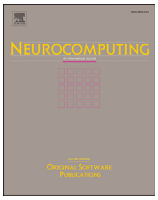

Fixed-time synchronization of octonion-valued neural networks with mixed delays: A non-separation norm approach

Vaibhav Agrawal [a], Sunny Singh [a, b,*], Vineet Kumar Singh [a], Subir Das [a]

[a] Department of Mathematical Sciences, Indian Institute of Technology (Banaras Hindu University), Varanasi 221005, India
[b] Faculty of Electrical Engineering, Mathematics and Computer Science, Delft University of Technology, Delft, 2628 CD, the Netherlands

ARTICLE INFO

Communicated by Q. Song

Keywords:
Fixed time synchronization
Projective synchronization
Mixed time delays
Lyapunov function
One norm
Octonion valued neural networks

ABSTRACT

This work emphasizes the fixed-time synchronization (FTS) of a specific class of octonion-valued neural networks (OVNNs), which incorporate discrete and distributed time delays. This study also establishes several norm properties for the octonion domains and explores FTS and fixed-time projective synchronization (FTPS) in OVNNs having mixed time delays by a suitable choice of the Lyapunov function, controllers and the one norm property. Unlike previous research on the decomposition of neural networks with octonion-valued and quaternion-valued components, this study introduces an enhanced one-norm method based on the non-separation approach. It employs a direct analytical approach to address two synchronization challenges using several norm properties. The computational complexity is reduced to provide less conservative results for OVNNs. This article analyzes various properties of the one norm of octonion domains and introduces effective controllers for achieving FTS and FTPS between the drive and response systems of OVNNs. The present article also establishes results in a compact and more generalized form using one norm criteria, which are easily verifiable to ensure synchronization, even with mixed time delays, which can be achieved within fixed time intervals. The settling time in each case illustrates its effectiveness compared to the existing results in a more straightforward way through a unique analytical process and more versatile activation functions. Finally, the theoretical results are validated through two numerical examples, with the overall results presented and discussed. Additionally, OVNNs are employed to demonstrate their effectiveness in storing and retrieving true-color images. This application showcases the ability of OVNNs to handle high-dimensional data representations, particularly in contexts where color channels and spatial features are strongly interrelated. The results highlight the robustness and efficiency of the proposed OVNNs framework, confirming its potential for advanced multidimensional data processing tasks.

1. Introduction

Artificial neural networks are designed to imitate how the human brain performs a particular task or action [1–6]. In recent years, there has been a growing interest among researchers in neural networks that operate with values in multidimensional domains, as mentioned in [7–11]. Complex-valued neural networks (CVNNs), initially introduced by Widrow et al. [12], have gained widespread applications. These applications include antenna design, radar imaging, estimation of direction of arrival and beamforming, image processing, communication signal processing, associative memory and more, as mentioned in [13–15]. In 1853, W.R. Hamilton first introduced Quaternion [16], a subset of Clifford algebra different from the real and complex domains. The commutativity law of multiplication does not apply to quaternions, one of their remarkable properties. Due to the non-commutativity inherent to quaternion algebra, progress in research within the quaternion domain has experienced a prolonged deceleration when contrasted with advancements in the real and complex fields. This is the primary reason for the slow research progress of QVNNs. Luckily, as modern mathematics has advanced and expanded, the applications of quaternions for future development have been discovered in recent years. Due to their potential applications in various fields, the research on quaternions has gained much attention, e.g., quaternions have good application prospects in three-dimensional wind forecasting [17], color face recognition [18], image compression [19,20] and quantum mechanics [21]. Quaternions often have excellent application prospects in 3D and 4D; an example of the utilization of quaternions to succinctly express spatial rotation

* Corresponding author at: Faculty of Electrical Engineering, Mathematics and Computer Science, Delft University of Technology, Delft, 2628 CD, the Netherlands
Email address: sunny.singh.rs.mat18@itbhu.ac.in (S. Singh).

https://doi.org/10.1016/j.neucom.2025.130995
Received 2 March 2025; Received in revised form 29 June 2025; Accepted 11 July 2025
Available online 16 July 2025

within the context of 3D geometrical affine transformations-translation can be provided [22]. Due to their promising applications, QVNNs have gained much attention in recent years [23–26].

However, with the advancement of technology, the quaternions and CVNNs fall short of fulfilling the demands of high-dimensional feature research. To address this limitation, quaternion and CVNNs have been extended to octonion-valued neural networks (OVNNs). The OVNNs were first introduced in 2016 [27], with activation functions, connection weights, states, and inputs being octonion numbers. As an extension, the OVNNs have more storage capacity and can carry more information. The octonion algebra, an extension of the complex and quaternion algebras, is 8-dimensional. Notably, it possesses the essential characteristic of being a normed division algebra, mathematically allowing the definition of both a norm and a multiplicative inverse. Interestingly, it can be demonstrated that the complex, quaternion, and octonion algebras are the exclusive normed division algebras that can be established over the field of real numbers. Unlike the commutative nature of the real and complex algebras, octonion algebra is both non-commutative and non-associative. This distinction sets it apart from the Clifford algebras, which are all associative. Until now, OVNNs have received limited attention, primarily due to the complexity of their structural analysis, which is mainly based on the present challenges for conventional separation approaches into eight equivalent real-valued neural networks given in [28–30]. While the separation approach is important, it can introduce complexities by necessitating handling eight systems instead of a single original system. This may compromise the originality of the proposed system. As of now, there have been relatively few results concerning OVNNs based on the non-separation approach, specifically considering discrete time delays given in [31–34]. Using the direct method, only a few studies have been addressed on FTS problems in OVNNs [28,35]. Many properties of octonion functions remain unexplored, indicating a need for further research and development. In most of the aforementioned results, synchronization can be achieved over an infinite period. Nonetheless, for practical applications, the synchronization errors often need to converge to the desired target within a finite time or limited timeframe to meet actual requirements. Finite-time synchronization has attracted much attention, as evidenced by references [36,37]. When employing a finite-time control scheme, the settling time is typically determined based on the initial values, which must be precisely known. However, this can be inconvenient in practice as the initial values may not always be available or accurate enough due to disturbances or uncertainties. Recognizing this limitation, Polyakov [38] has removed this shortcoming by giving a new concept known as fixed time, which is independent of all initial values. The fixed-time concept sets a uniform fixed upper bound for the settling time, independent of all initial values. This characteristic offers significant convenience in practical applications. Due to this advancement in finite-time concepts, fixed time is a trending concept these days. The fixed-time approach has gained popularity in the control field in recent years, mainly in the higher-dimensional domain, as evidenced by references [4,25,39–45]. Inspired by the preceding description, there is significance in efficiently synchronizing the intricate dynamic behaviour of high-dimensional data systems with delays, such as those found in secure communication [46,47] and image compression systems [23,48], within a fixed or finite time framework. In practical applications like network control systems, time delays are frequently encountered. These time delays stem from hardware limitations in switching speed, signal transmission interferences due to faults, and other factors. It is crucial to note that these delays can exacerbate the system's dynamic performance,which will potentially lead to instability, oscillations, bifurcations, or even chaotic behaviour. This issue is unavoidable in the deployment of artificial neural networks. In neural networks, mixed time delays play an important role, and it is more general and significant to consider mixed time delays in the model. Therefore, it is imperative to investigate the dynamic behaviours of OVNNs with mixed kinds of time-varying delays. To the best of the authors' knowledge, the research on the investigation of FTS and FTPS has not yet been done with mixed time delays for OVNNs without employing separation techniques and one norm property. This observation promotes exploring effective methods to ensure FTS and FTPS through a direct approach. Inspired by this analysis, the main innovative contributions of the present article are given as follows:

1. Most OVNNs are decomposed into eight RVNNs using the decomposition method, which requires the calculation and proof process to be performed using Lyapunov analysis eight times. Consequently, utilizing the non-decomposition method based on the one norm simplifies the calculation process and increases precision. Hence, our proposed methods are less conservative as compared to some existing research works on the octonion domain [28,49].
2. An enhanced and improved one-norm method has proved to be universal and effective in addressing FTS and FTPS problems of OVNNs. This non-decomposition method involves rewriting the one-norm of an octonion by introducing the sign function. The Lyapunov function and controller are constructed using the improved one-norm. The derivative terms of the Lyapunov functional are then scaled using certain inequalities of the one-norm of the octonion to complete the Lyapunov analysis.
3. The proposed results are validated through two numerical examples, demonstrating the effectiveness and efficiency of the approach. Furthermore, if the decomposition of the activation function is restricted utilizing the one-norm, it is an effective strategy to address this challenge. Consequently, our proposed method is less conservative than existing approaches.

The remainder of this paper can be outlined as follows: In Section 2, we introduce the preliminaries and model formulation for OVNNs along with pertinent definitions and lemmas. The primary findings, encompassing FTS and FTPS, are expounded upon in Section 3. Section 4 showcases numerous numerical simulations that corroborate the principal outcomes. Finally, Section 5 provides a brief conclusion and outlines potential avenues for future research.

Notations: The sets of real numbers and non-negative real numbers are denoted by $\mathbb{R}$ and $\mathbb{R}^+$, respectively. The set of all octonions is represented by $\mathbb{O}$. Superscripts T and $*$ stand for transposition and conjugate transpose, respectively. The sets of all n-dimensional real numbers, complex numbers, quaternion numbers, and octonions are represented by $\mathbb{R}^n$, $\mathbb{C}^n$, $\mathbb{H}^n$, and $\mathbb{O}^n$. The one-norm is denoted by $|\cdot|_1$ and the sign function by $\mathrm{sgn}(\cdot)$. The sets $\mathbb{R}^{n\times m}$, $\mathbb{C}^{n\times m}$, and $\mathbb{O}^{n\times m}$ denote $n\times m$ matrices with real, complex, and octonion entries, respectively. Real numbers, complex numbers, and quaternions are special cases of octonions (i.e., $\mathbb{R}\subset\mathbb{C}\subset\mathbb{H}\subset\mathbb{O}$).

$\psi \in C\left([-\overline{\tau},0],\mathbb{O}^M\right)$ denotes a continuous map whose domain and range are $[-\overline{\tau},0]$ and $\mathbb{O}^M$, respectively. The one-norm of vector $\upsilon = \left(\upsilon_1,\upsilon_2,\ldots,\upsilon_n\right) \in \mathbf{R}^n$ and the octonion $\boldsymbol{x}$ are written as $\|\upsilon\|_1 = \Sigma_{p=1}^n\|\upsilon_p\|$ and $\|\boldsymbol{x}\|_1 = \Sigma_{\zeta=0,1,\ldots,7}\|x_{(\zeta)}\|_1$, respectively. For $\boldsymbol{e}(t) = \left(\boldsymbol{e}_1(t),\boldsymbol{e}_2(t),\ldots,\boldsymbol{e}_n(t)\right)^T \in \mathbb{O}^n$, the sign function and one-norm of vector $\boldsymbol{e}(t)$ are denoted by $\mathrm{sgn}(\boldsymbol{e}(t)) = \left(\mathrm{sgn}\left(\boldsymbol{e}_1(t)\right),\mathrm{sgn}\left(\boldsymbol{e}_2(t)\right),\ldots,\mathrm{sgn}\left(\boldsymbol{e}_n(t)\right)\right)^T$, $\|\boldsymbol{e}(t)\|_1 = \Sigma_{p=1}^n\|\boldsymbol{e}_p(t)\|_1$, respectively. Again $[\boldsymbol{e}(t)]^m = \left(\left[\boldsymbol{e}_1(t)\right]^m,\left[\boldsymbol{e}_2(t)\right]^m,\ldots,\left[\boldsymbol{e}_n(t)\right]^m\right)^T$, with $\left[\boldsymbol{e}_p(t)\right]^m = \mathrm{sgn}\left(\boldsymbol{e}_p(t)\right)\|\boldsymbol{e}_p(t)\|_1^m, p=1,2,\ldots,n$ and $m>0, I=\{1,2,\ldots,M\}$.

2. Preliminaries and model formulation

2.1. Octonions algebra

The octonion $\mathbb{O}$ is an 8-dimensional algebra with the basis $\{w_0,w_1,\ldots,w_7\}$. In this algebra, $w_0=1$ and w_j for $j=1,2,\ldots,7$, represent the octonion generators. These generators adhere to the following rules

$$\begin{cases} w_j w_k = -w_k w_j, & \text{for } j \neq k, \\ w_j^2 = -1, & \text{for } j = 1, 2, \dots, 7, \\ w_0^2 = 1. \end{cases}$$

The set of all octonions, denoted by $\mathbb{O}$, is defined as

$$\mathbb{O} := \left\{ p = \Sigma_{j=0}^{7}\, p^{(j)} w_j \;\middle|\; p^{(j)} \in \mathbb{R},\ j = 0, 1, \dots, 7 \right\},$$

Since it is defined over the real field $\mathbb{R}$, it can be considered a real octonion.

The modulus of $\boldsymbol{p}$ is defined as

$$|p| = \sqrt{p\overline{p}} = \sqrt{(p^{(0)})^2 + (p^{(1)})^2 + (p^{(2)})^2 + (p^{(3)})^2 + (p^{(4)})^2 + (p^{(5)})^2 + (p^{(6)})^2 + (p^{(7)})^2}.$$

The transpose of the vector $\boldsymbol{p}$ is denoted by $\boldsymbol{p}^T$, and the conjugate and conjugate transpose of $\boldsymbol{p}$ are denoted by $\overline{\boldsymbol{p}} = p^{(0)}w_0 - p^{(1)}w_1 - p^{(2)}(t)w_2 - \cdots - p^{(7)}(t)w_7$ and $\boldsymbol{p}^* = p^{(0)}(t)^T w_0 - p^{(1)}(t)^T w_1 - p^{(2)}(t)^T w_2 - \cdots - p^{(7)}(t)^T w_7$, respectively.

For any two octonions p, y

$$\boldsymbol{p} = p^{(0)}w_0 + p^{(1)}w_1 + p^{(2)}w_2 + \cdots + p^{(7)}w_7,$$
$$\boldsymbol{y} = y^{(0)}w_0 + y^{(1)}w_1 + y^{(2)}w_2 + \cdots + y^{(7)}w_7,$$

the addition of $p + y$ is defined as

$$\boldsymbol{p}+\boldsymbol{y} = \left(p^{(0)} + y^{(0)}\right) w_0 + \left(p^{(1)} + y^{(1)}\right) w_1 + \left(p^{(2)} + y^{(2)}\right) w_2 + \cdots + \left(p^{(7)} + y^{(7)}\right) w_7.$$

and the scaler multiplication is defined as

$$a\boldsymbol{p} = \Sigma_{j=0}^{7}(ap^{(j)})w_j, \forall a \in \mathbb{R}.$$

2.2. Preliminaries and model description

Let us consider the OVNNs with mixed time delays as

$$\dot{x}_r(t) = -a_r x_r(t) + \Sigma_{j=1}^{M} b_{rj} f_j(x_j(t)) + \Sigma_{j=1}^{M} c_{rj} g_j(x_j(t - \tau_{rj}(t))) + \Sigma_{j=1}^{M} d_{rj} \int_{t-\sigma_{rj}(t)}^{t} h_j(x_j(s))ds, \quad (1)$$

where $r \in I, x_r(t) \in \mathbb{O}$ is the state variable, $a_r > 0$, b_{rj}, c_{rj} and d_{rj} are the octonion weight connection matrices,

$\mathcal{F} = f, g, h$ are the octonion activation functions and $\tau_{rj}(t)$ is the discrete delay while $\sigma_{rj}(t)$ is the distributed delay that satisfies the inequality $0 < |\dot{\tau}_{rj}(t)|, |\dot{\sigma}_{rj}(t)| \leq 1$.

Let $x(s) = \phi(s) \in \mathbb{O}^M$,and $s \in [\overline{\tau}, 0]$ is the initial condition of the system, where $\phi(s) = \phi^0(s)w_0 + \phi^1(s)w_1 + \cdots + \phi^7(s)w_7$, with $\overline{\tau} = \max\{\tau_{rj}(t), \sigma_{rj}(t)\}$.

Remark 1. Given that the absolute value of a real number x can be expressed as $|x| = xsgn(x)$, and the one-norm of a complex number $z = z_R + iz_I$ (where z_R and z_I belong to $\mathbb{R}$) can be represented as $\|z\|_1 = \|z_R\|_1 + \|z_I\|_1 = \frac{1}{2}\left(\text{sgn}(z) \cdot z^* + \text{sgn}(z)^* \cdot z\right)$. Motivated by this, the sign function has been incorporated into the enhanced one-norm of octonion considered in the present article. This inclusion is pivotal for the subsequent discussions. The proof is straightforward and therefore omitted.

Remark 2. In the present article, the FTS and FTPS results have been investigated by utilizing the norm property without the separation approach, which has significantly reduced the computational complexity. The conditions of the theorems are easily satisfied by using the norm property.

Assumption 1. For any $x_j(t), y_j(t) \in \mathbf{O}$ and $j = 1, 2, \dots, M$, suppose the activation functions are

$\hat{f}_j(x_j(t)) : \hat{f}_j(x_j(t)) = \hat{f}_j(x_j(t))^0 w_0 + \hat{f}_j(x_j(t))^1 w_1 + \cdots + \hat{f}_j(x_j(t))^7 w_7$ such that $\hat{f}_j(0) = 0$,

$\hat{g}_j(x_j(t)) : \hat{g}_j(x_j(t)) = \hat{g}_j(x_j(t))^0 w_0 + \hat{g}_j(x_j(t))^1 w_1 + \cdots + \hat{g}_j(x_j(t))^7 w_7$ such that $\hat{g}_j(0) = 0$ and $\hat{h}_j(x_j(t)) : \hat{h}_j(x_j(t)) = \hat{h}_j(x_j(t))^0 w_0 + \hat{h}_j(x_j(t))^1 w_1 + \cdots + \hat{h}_j(x_j(t))^7 w_7$ such that $\hat{h}_j(0) = 0$, where

$\hat{f}_j(x_j(t))^\mu = \hat{f}_j^\mu(x_j^0(t), x_j^1(t), \dots, x_j^7(t))$, $\hat{g}_j(x_j(t))^\mu = \hat{g}_j^\mu(x_j^0(t), x_j^1(t), \dots, x_j^7(t))$ and $\hat{h}_j(x_j(t))^\mu = \hat{h}_j^\mu(x_j^0(t), x_j^1(t), \dots, x_j^7(t))$, $\mu = 0, 1, \dots 7$,

and there exist positive constants $F_j, G_j$and $H_j > 0$ which satisfy the following inequalities:

$$\|\hat{f}_j(y_j(t)) - \hat{f}_j(x_j(t))\|_1 \leq F_j \|y_j(t) - x_j(t)\|_1,$$
$$\|\hat{g}_j(y_j(t)) - \hat{g}_j(x_j(t))\|_1 \leq G_j \|y_j(t) - x_j(t)\|_1,$$
$$\|\hat{h}_j(y_j(t)) - \hat{h}_j(x_j(t))\|_1 \leq H_j \|y_j(t) - x_j(t)\|_1.$$

Lemma 1 ([50]). *Suppose $0 \leq \alpha \leq 1$ and $\beta > 1$; then for any $z_j \in \mathbb{R}_+ (j \in I)$, satisfies the inequalities $\Sigma_{j=1}^{M} z_j^\alpha \geq \left(\Sigma_{j=1}^{M} z_j\right)^\alpha$ and $\Sigma_{j=1}^{M} z_j^\beta \geq M^{1-\beta}\left(\Sigma_{j=1}^{M} z_j\right)^\beta$.*

Lemma 2 ([35]). *Suppose $u(t) = (u_1(t), u_2(t), \dots, u_M(t))^T, v(t) = (v_1(t), v_2(t), \dots, v_M(t))^T \in \mathbf{O}^M$ and $u(t) = u^0(t)\, w_0 + u^1(t)\, w_1 + u^2(t)\, w_2 + \cdots + u^7(t) w_7$ and $v(t) = v^0(t)\, w_0 + v^1(t)\, w_1 + v^2(t)\, w_2 + \cdots + v^7(t)\, w_7$, where $u_r(t), v_r(t) \in \mathbf{O}$, $r = 1, 2, \dots, M$, and $u^\mu(t), l^\mu(t) \in \mathbb{R}^M, \mu = 0, 1, 2, \dots, 7$, then for $u(t), v(t) \in \mathbf{O}^M, a \leq b$, and $q > 0$, the following formulas hold*

(1) $u(t)^* sgn(v(t)) + sgn(v(t))^* u(t) \leq u(t)^* sgn(u(t)) + sgn(u(t))^* u(t) = 2\|u(t)\|_1$

(2) $D^+\left(u(t)^* sgn(u(t)) + sgn(u(t))^* u(t)\right) = sgn(u(t))^* \dot{u}(t) + u(t)^* sgn(\dot{u}(t))$

(3) $\|u(t)^T v(t)\|_1 \leq \|u(t)\|_1 \|v(t)\|_1$

(4) $sgn(u(t))^* sgn(u(t)) = \|sgn(u(t))\|_1$

(5) $\left\|\int_a^b g(u(t))dt\right\|_1 \leq \int_a^b \|g(u(t))\|_1 ds$

(6) $sgn(u(t))^*[u(t)]^q + \left([u(t)]^q\right)^* sgn(u(t)) = 2\|[u(t)]^q\|_1 \geq \begin{cases} 2\, M^{1-q}\|u(t)\|_1^q, & q > 1 \\ 2\|u(t)\|_1^q, & 0 < q \leq 1. \end{cases}$

Proof. Based on the given conditions, one can derive

(1) $u(t)^* sgn(v(t)) + sgn(v(t))^* u(t)$

$= \left(u^0(t)^T w_0 - u^1(t)^T w_1 - u^2(t)^T w_2 - \cdots - u^7(t)^T w_7\right)$
$\times \left(sgn(v^0(t))w_0 + sgn(v^1(t))w_1 + sgn(v^2(t))w_2 + \cdots + sgn(v^7(t))w_7\right) + \left(sgn(v^0(t))\, w_0 - sgn(v^1(t))\, w_1 - sgn(v^2(t))w_2 - \cdots - sgn(v^7(t))w_7\right) \times \left(u^0(t)^T w_0 + u^1(t)^T w_1 + u^2(t)^T w_2 + \cdots + u^7(t)^T w_7\right)$

$= 2\left(u^0(t)^T w_0\ sgn(v^0(t)) + u^1(t)^T\ sgn(v^1(t)) + u^2(t)^T\ sgn(v^2(t)) + \ldots + u^7(t)^T\ sgn(v^7(t))\right)$

$\leq 2\left(\|u^0(t)w_0\|_1 + \|u^1(t)\|_1 + \|u^2(t)\|_1 + \cdots + \|u^7(t)\|_1\right)$

$= 2\|u(t)\|_1$ **(Proved)**.

Taking the upper right Dini derivative of condition 2, we get

(2) $D^+\left(u(t)^* sgn(u(t)) + sgn(u(t))^* u(t)\right) = 2sgn\left(\|u(t)\|_1\right)\frac{d\|u(t)\|_1}{dt}$

$= 2\frac{d\|u(t)\|_1}{dt} = 2\Sigma_{r=1}^{M}\left(sgn\left((u_r^0(t)w_0\right)^T \frac{du_r^0(t)}{dt} + \left(sgn\left((u_r^1(t)\right)^T \frac{du_r^1(t)}{dt} + \left(sgn\left((u_r^2(t)\right)^T \frac{du_r^2(t)}{dt} + \cdots + \left(sgn\left((u_r^7(t)\right)^T \frac{du_r^7(t)}{dt}\right)$

$= sgn(u(t))^* \dot{u}(t) + u(t)^* sgn(\dot{u}(t))$. **(Proved)**

(3) $\|u(t)^T v(t)\|_1$

$$= \left\| \begin{array}{l} \left(u^0(t)^T w_0 + u^1(t)^T w_1 + u^2(t)^T w_2 + \cdots + u^7(t)^T w_7\right) \times \\ \left(v^0(t)^T w_0 + v^1(t)^T w_1 + v^2(t)^T w_2 + \cdots + v^7(t)^T w_7\right) \end{array} \right\|_1$$

$$= \left\| \begin{array}{l} w_0\left(u^0(t)^T v^0(t) - u^1(t)^T v^1(t) - u^2(t)^T v^2(t) - u^3(t)^T v^3(t) - u^4(t)^T v^4(t)\right. \\ \left. -u^5(t)^T v^5(t) - u^6(t)^T v^6(t) - u^7(t)^T v^7(t)\right) + \\ w_1\left(u^0(t)^T v^1(t) + u^1(t)^T v^0(t) + u^2(t)^T v^3(t) - u^3(t)^T v^2(t) + u^4(t)^T v^5(t)\right. \\ \left. -u^5(t)^T v^4(t) - u^6(t)^T v^7(t) + u^7(t)^T v^6(t)\right) + \\ w_2\left(u^0(t)^T v^2(t) - u^1(t)^T v^3(t) + u^2(t)^T v^0(t) + u^3(t)^T v^1(t) + u^4(t)^T v^6(t)\right. \\ \left. +u^5(t)^T v^7(t) - u^6(t)^T v^4(t) - u^7(t)^T v^5(t)\right) + \\ w_3\left(u^0(t)^T v^3(t) + u^1(t)^T v^2(t) - u^2(t)^T v^1(t) + u^3(t)^T v^0(t) + u^4(t)^T v^7(t)\right. \\ \left. -u^5(t)^T v^6(t) + u^6(t)^T v^5(t) - u^7(t)^T v^4(t)\right) + \\ w_4\left(u^0(t)^T v^4(t) - u^1(t)^T v^5(t) - u^2(t)^T v^6(t) - u^3(t)^T v^7(t) + u^4(t)^T v^0(t)\right. \\ \left. +u^5(t)^T v^1(t) - u^6(t)^T v^2(t) - u^7(t)^T v^3(t)\right) + \\ w_5\left(u^0(t)^T v^5(t) + u^1(t)^T v^4(t) - u^2(t)^T v^7(t) + u^3(t)^T v^6(t) - u^4(t)^T v^1(t)\right. \\ \left. +u^5(t)^T v^0(t) - u^6(t)^T v^3(t) + u^7(t)^T v^2(t)\right) + \\ w_6\left(u^0(t)^T v^6(t) + u^1(t)^T v^7(t) + u^2(t)^T v^4(t) - u^3(t)^T v^5(t) - u^4(t)^T v^2(t)\right. \\ \left. +u^5(t)^T v^3(t) + u^6(t)^T v^0(t) - u^7(t)^T v^1(t)\right) + \\ w_7\left(u^0(t)^T v^7(t) - u^1(t)^T v^6(t) + u^2(t)^T v^5(t) + u^3(t)^T v^4(t) - u^4(t)^T v^3(t)\right. \\ \left. -u^5(t)^T v^7 2(t) + u^6(t)^T v^1(t) + u^7(t)^T v^0(t)\right) \end{array} \right\|_1$$

$$\leq |w_0|\Big(|u^0(t)^T v^0(t)| + |u^1(t)^T v^1(t)| + |u^2(t)^T v^2(t) + |u^3(t)^T v^3(t)| + |u^4(t)^T v^4(t)| + |u^5(t)^T v^5(t)| + |u^6(t)^T v^6(t)| + |u^7(t)^T v^7(t)|\Big) + \Big(|u^0(t)^T v^1(t)| + |u^1(t)^T v^0(t)| + |u^2(t)^T v^3(t)| + |u^3(t)^T v^2(t)| + |u^4(t)^T v^5(t)| + |u^5(t)^T v^4(t)| + |u^6(t)^T v^7(t)|\Big) + \Big(|u^7(t)^T v^6(t)| + |u^0(t)^T v^2(t)| + |u^1(t)^T v^3(t)| + |u^2(t)^T v^0(t)| + |u^3(t)^T v^1(t)| + |u^4(t)^T v^6(t)| + |u^5(t)^T v^7(t)| + |u^6(t)^T v^4(t)|\Big) + \Big(|u^7(t)^T v^5(t)| + |(u^0(t)^T v^2(t)| + |u^1(t)^T v^3(t)| + |u^2(t)^T v^0(t)| + |u^3(t)^T v^1(t)| + |u^4(t)^T v^6(t)| + |u^5(t)^T v^7(t)|\Big) + \Big(|u^6(t)^T v^4(t)| + |u^7(t)^T v^5(t)| + |u^0(t)^T v^3(t)| + |u^1(t)^T v^2(t)| + |u^2(t)^T v^1(t)| + |u^3(t)^T v^0(t)| + |u^4(t)^T v^7(t)|\Big) + \Big(|u^5(t)^T v^6(t)| + |u^6(t)^T v^5(t)| + |u^7(t)^T v^4(t)| + |u^0(t)^T v^4(t)| + |u^1(t)^T v^5(t)| + |u^2(t)^T v^6(t)| + |u^3(t)^T v^7(t)|\Big) + \Big(|u^4(t)^T v^0(t)| + |u^5(t)^T v^1(t)| + |u^6(t)^T v^2(t)| + |u^7(t)^T v^3(t)| + |u^0(t)^T v^5(t)| + |u^1(t)^T v^4(t| + |u^2(t)^T v^7(t)|\Big) + \Big(|u^3(t)^T v^6(t)| + |u^4(t)^T v^1(t)| + |u^5(t)^T v^0(t)| + |u^6(t)^T v^3(t)| + |u^7(t)^T v^2(t)| + |u^0(t)^T v^6(t)| + |u^1(t)^T v^7(t)|\Big) + \Big(|u^2(t)^T v^4(t)| + |u^3(t)^T v^5(t)| + |u^4(t)^T v^2(t)| + |u^5(t)^T v^3(t)| + |u^6(t)^T v^0(t)| + |u^7(t)^T v^1(t)| + |u^0(t)^T v^7(t)|\Big) + \Big(|u^1(t)^T v^6(t)| + |u^2(t)^T v^5(t)| + |u^3(t)^T v^4(t)| + |u^4(t)^T v^3(t)| + |u^5(t)^T v^2(t)| + |u^6(t)^T v^1(t)| + |u^7(t)^T v^0(t)|\Big)$$

$$\leq |w_0|\Big(|u_1^o(t)v_1^0(t)| + |u_2^o(t)v_2^0(t)| + \cdots + |u_M^o(t)v_M^0(t)|\Big) + \Big(|u_1^1(t)v_1^1(t)| + |u_2^1(t)v_2^1(t)| + \cdots + |u_M^1(t)v_M^0(t)|\Big) + \Big(|u_1^2(t)v_1^2(t)| + |u_2^2(t)v_2^2(t)| + \cdots + |u_M^2(t)v_M^2(t)|\Big) + \cdots + \Big(|u_1^7(t)v_1^7(t)| + |u_2^7(t)v_2^7(t)| + \cdots + |u_M^7(t)v_M^7(t)|\Big) \leq ||u(t)||_1 \|v(t)\|_1$. **(Proved)**

(4) $sgn(u(t))^*(sgn(u(t)) = \Big(sgn(u_0(t))^T w_0 - sgn(u_1(t))^T w_1 - sgn(u_2(t))^T w_2 - sgn(u_3(t))^T w_3 - sgn(u_4(t))^T w_4 - sgn(u_5(t))^T w_5 - sgn(u_6(t))^T w_6 - sgn(u_7(t))^T w_7\Big) \times \Big(sgn(u_0(t))^T w_0 + sgn(u_1(t))^T w_1 + sgn(u_2(t))^T w_2 + sgn(u_3(t))^T w_3 + sgn(u_4(t))^T w_4 + sgn(u_5(t))^T w_5 + sgn(u_6(t))^T w_6 + sgn(u_7(t))^T w_7\Big)$

$= \|sgn(u^0(t))w_0\|_1 + \|sgn(u^1(t))\|_1 + \cdots + \|sgn(u^7(t))\|_1$

$= \|sgn(u(t))\|_1$. **(Proved)**

(5) $\left\| \int_a^b g(u(t))\, dt \right\|_1$

$$= \left\| \int_a^b \left(g^{(0)}(u(t))w_0 + g^{(1)}(u(t))w_1 + \cdots + g^{(7)}(u(t))w_7\right) dt \right\|_1$$

$$\leq \left\| \int_a^b g^{(0)}(u(t))w_0\, dt \right\|_1 + \left\| \int_a^b g^{(1)}(u(t))w_1\, dt \right\|_1 + \cdots + \left\| \int_a^b g^{(7)}(u(t))w_7\, dt \right\|_1$$

$$\leq \left\| \int_a^b g_1^{(0)}(u_1(t))\, dt \right\|_1 + \left\| \int_a^b g_2^{(0)}(u_2(t))\, dt \right\|_1 + \cdots + \left\| \int_a^b g_M^{(0)}(u_M(t))\, dt \right\|_1 + \left\| \int_a^b g_1^{(1)}(u_1(t))\, dt \right\|_1 + \left\| \int_a^b g_2^{(1)}(u_2(t))\, dt \right\|_1 + \cdots + \left\| \int_a^b g_M^{(1)}(u_M(t))\, dt \right\|_1 + \cdots + \left\| \int_a^b g_1^{(7)}(u_1(t))\, dt \right\|_1 + \left\| \int_a^b g_1^{(7)}(u_1(t))\, dt \right\|_1 \cdots + \left\| \int_a^b g_M^{(7)}(u_M(t))\, dt \right\|_1$$

$$\leq \int_a^b \left\|g^{(0)}(u(t))w_0\right\|_1 dt + \int_a^b \left\|g^{(1)}(u(t))w_1\right\|_1 dt + \cdots + \int_a^b \left\|g^{(7)}(u(t))w_7\right\|_1 dt.$$

$$= \int_a^b \left\|g(u(t))\right\|_1 dt.$$ **(Proved)**

From the Lemma 1, it can be easily observed that $\|sgn(u_s(t))\|_1 \geq 1$, if $u_s(t) \neq 0, and \|sgn(u_s(t))\|_1 = 0$ for $u_s(t) = 0$ and it can be obtained.

(6) $sgn(u(t))^*[u(t)]^q + ([u(t)]^q)^* sgn(u(t))$

$= sgn(u_1(t))^* sgn(u_1(t))\|u_1(t)\|_1^q + \cdots + sgn(u_M(t))^* sgn(u_M(t))\|u_M(t)\|_1^q + sgn(u_1(t))^* sgn(u_1(t))\|u_1(t)\|_1^q + \cdots + sgn(u_M(t))^* sgn(u_M(t))\|u_M(t)\|_1^q$

$= 2\Big(sgn(u_1(t))^* sgn(u_1(t))\|u_1(t)\|_1|^q + \cdots + sgn(u_M(t))^* sgn(u_M(t))\|u_M(t)\|_1^q\Big)$

$= 2\Big(\|sgn(u_1(t))\|u_1(t)\|_1^q\|_1 + \cdots + \|sgn(u_M(t))\|u_M(t)\|_1^q\|_1\Big)$

$= 2\|[u(t)]^q\|_1$

$$\geq \begin{cases} 2\, M^{1-q}\|u(t)\|_1^q, & q > 1 \\ 2\|u(t)\|_1^q, & 0 < q \leq 1. \end{cases}$$ **(Proved)**

□

Remark 3. The conclusion drawn from Lemma 2 can be extended to 1D octonion, underscoring the practicality of the Lemma. In future endeavors, one can explore the scenario where $v_r(t)$ represents an n-dimensional vector in $\mathbb{O}$ (where $n \in \mathbb{R}^+$), and subsequently, all the derivations presented in this article remain applicable.

Remark 4. Lemma 2 makes it evident that the one-norm of $u(t)$ belonging to $\mathbb{O}^M$ can be derived as $\|u(t)\|_1 = \frac{1}{2}\left(\text{sgn}(u(t))^* u(t) + u(t)^* \text{sgn}(u(t))\right)$. Lemma 2 illustrates that by incorporating the sign function $\text{sgn}(u(t))$, we can seamlessly convert an octonion expression into a real-valued one-norm.

Let us consider Eq. (1) as the master system, and the corresponding response systems are described as

$$\dot{y}_r(t) = -a_r y_r(t) + \Sigma_{j=1}^M b_{rj} f_j(y_j(t)) + \Sigma_{j=1}^M c_{rj} g_j(y_j(t - \tau_{rj}(t))) + \Sigma_{j=1}^M d_{rj} \int_{t-\sigma_{rj}(t)}^t h_j(y_j(s))ds + U_r(t), \quad (2)$$

where all the parameters are the same as in Eq. (1), $U_r(t)$ is the controller, where $r \in I$ and $y(s) = \psi(s) \in C\left([-\overline{\tau}, 0], \mathbb{O}^M\right)$ is the initial condition.

The synchronization error is defined as $e_r(t) = y_r(t) - x_r(t)$, for $r \in I$.

Using the equations of master and response systems in the above equation, we have the error equation as

$$\dot{e}_r(t) = -a_r e_r(t) + \Sigma_{j=1}^{M} b_{rj}\hat{f}_j(e_j(t)) + \Sigma_{j=1}^{M} c_{rj}\hat{g}_j(e_j(t-\tau_{rj}(t))) + \Sigma_{j=1}^{M} d_{rj}\int_{t-\sigma_{rj}(t)}^{t} \hat{h}_j(e_j(s))ds + U_r(t), \tag{3}$$

where $\mathcal{F}_j(e_j(t)) = \mathcal{F}_j(y_j(t)) - \mathcal{F}_j(x_j(t))$, and $\mathcal{F} = f, g, h$ and $j \in I$ also $e(s) = \Phi(s) = \psi(s) - \phi(s) \in C\left([-\overline{\tau}, 0], \mathbb{O}^M\right)$.

Definition 1 ([38]). The master system (1) and response system (2) are synchronized within the finite time if the error system is synchronized within the finite time, and settling time depends on the initial conditions.

For any solution $e(t)$ starting at e_0, it is asymptotically stable, and $\lim_{t\to T(e_0)} \|e(t)\| = 0$ holds, with $e(t) = 0$ for all $t \geq T_0$, where T_0 is referred to as the settling time function.

Definition 2 ([38]). The master system (1) and response system (2) are fixed time synchronized if the error system is synchronized within the finite time and the settling time is independent of the initial conditions.

An equilibrium point is termed fixed-time stable if it satisfies the conditions of finite-time stability and the settling time is uniformly bounded, i.e., $T(e_0) < T_{\max}$ for all e_0, where $T_{\max}$ is a constant.

Lemma 3 ([38]). *Assume that there exists a continuous, radially unbounded function $V : \mathbf{R}^n \to \mathbf{R}^+ = [0, +\infty)$ satisfying:*

1. *$V(\mathbf{e}(t)) = 0$ if and only if $\mathbf{e}(t) = 0$,*
2. *$\frac{d}{dt}V(\mathbf{e}(t)) \leq -aV^{\alpha}(\mathbf{e}(t)) - bV^{\beta}(\mathbf{e}(t))$, where $a, b > 0$, $0 < \alpha < 1$, and $\beta > 1$.*

Then the origin of the error system (3) is fixed-time stable, and $V(\mathbf{e}(t)) = 0$ for $t \geq T(\mathbf{e}_0)$, where the settling time $T(\mathbf{e}_0)$ is bounded by

$$T(\mathbf{e}_0) \leq T_{\max} = \frac{1}{a}\left(\frac{a}{b}\right)^{\frac{1-\alpha}{\beta-\alpha}}\left(\frac{1}{\beta-1} + \frac{1}{1-\alpha}\right), \quad \text{for all } \mathbf{e}_0 \in \mathbf{R}^n.$$

Remark 5 ([38]). Under the same conditions as in Lemma 3, the synchronization time $T(\mathbf{e}_0)$ can also be estimated by the following formula

$$T(\mathbf{e}_0) \leq T_{\max} = \frac{1}{a(1-\alpha)} + \frac{1}{b(\beta-1)}, \ \forall\ \mathbf{e}_0 \in \mathbf{R}^n.$$

3. Main result

This section examines the FTS and FTPS for OVNNs with mixed delays. By utilizing the derived norm properties presented in Section 2 in the form of Lemmas, we propose an alternative approach to the stability analysis of higher-dimensional neural networks. To enhance the clarity and understanding for readers, we have divided this section into two subsections:

- Section 3.1 focuses exclusively on the study of FTS.
- Section 3.2 addresses the study of FTPS.

3.1. FTS result for master and response systems

This structure ensures a more systematic and comprehensive presentation of the results. To achieve FTS for OVNNs with mixed time delays between the master and response systems, let us use the novel controller based on the one-norm as

$$U_r(t) = \rho_{1r}e_r(t) - \rho_{2r}(e_r(t))^{\alpha} - \rho_{3r}(e_r(t))^{\beta} + \rho_{4r}\Sigma_{j=1}^{M} e_r(t-\tau_{rj}(t)) + \rho_{5r}\Sigma_{j=1}^{M}\int_{t-\sigma_{rj}(t)}^{t} \|e_j(s)\|_1 ds, \tag{4}$$

where $\rho_{1r}, \rho_{2r}, \rho_{3r}, \rho_{4r}$ are the control parameters which are determined later, and $0 < \alpha < 1, \beta > 1$.

Theorem 1. *Assuming that Assumption 1 holds and if the parameters $\rho_{1r}, \rho_{2r}, \rho_{3r}, \rho_{4r}$ and ρ_{5r} in the controller (4) satisfy the following conditions*

$$-a_r + \rho_{1r} + \Sigma_{j=1}^{M}\|b_{jr}\|_1 F_r \leq 0,$$

$$\Sigma_{j=1}^{M}\left(\|c_{jr}\|_1 G_r + \rho_{4j}G_r\right) \leq 0,$$

$$\Sigma_{j=1}^{M}\|d_{rj}\|_1 H_j + \rho_{5r} \leq 0,\ \rho_{2r} > 0,\ \rho_{3r} > 0,$$

$\forall\ r \in I$, then the drive system (1) synchronizes to the corresponding response system (2) in a fixed time, and the corresponding settling time is estimated as

$$T_1 = \frac{1}{\rho_2}\left(\frac{\rho_2}{M^{2(1-\beta)}\rho_3}\right)^{\frac{1-\alpha}{\beta-\alpha}}\left(\frac{1}{\beta-1} + \frac{1}{1-\alpha}\right), \tag{5}$$

where $\rho_2 = \min_{1\leq r\leq M}\{\rho_{2r}\}$, $\rho_3 = \min_{1\leq r\leq M}\{\rho_{3r}\}$.

Proof. Let us construct the appropriate Lyapunov function as

$$V(t) = \frac{1}{2}\Sigma_{r=1}^{M}\left(sgn(e_r(t))^* e_r(t) + e_r(t)^* sgn(e_r(t))\right). \tag{6}$$

Taking derivative of $V(t)$ with respect to t along the error Eq. (3), one can get

$$\begin{aligned} D^+V(t) &= \frac{1}{2}\Sigma_{r=1}^{M}\left(sgn(e_r(t))^*\dot{e}_r(t) + \dot{e}_r(t)^* sgn(e_r(t))\right) \\ &= \frac{1}{2}\Sigma_{r=1}^{M} sgn(e_r(t))^*\Bigg(- a_r e_r(t) \\ &\quad + \Sigma_{j=1}^{M} b_{rj}\hat{f}_j(e_j(t)) + \Sigma_{j=1}^{M} c_{rj}\hat{g}_j(e_j(t-\tau_{rj}(t))) \\ &\quad + \Sigma_{j=1}^{M} d_{rj}\int_{t-\sigma_{rj}}^{t}\hat{h}_j(e_j(s))ds + \rho_{1r}e_r(t) - \rho_{2r}(e_r(t))^{\alpha} - \rho_{3r}(e_r(t))^{\beta} \\ &\quad + \rho_{4r}\Sigma_{j=1}^{M} e_r(t-\tau_{rj}(t)) + \rho_{5r}\Sigma_{j=1}^{M}\int_{t-\sigma_{rj}(t)}^{t}\|e_j(s)\|_1 ds\Bigg) \\ &\quad + \frac{1}{2}\Sigma_{r=1}^{M}\Bigg(- a_r e_r^*(t) + \Sigma_{j=1}^{M}(\hat{f}_j(e_j(t)))^* b_{rj}^* \\ &\quad + \Sigma_{j=1}^{M}(\hat{g}_j(e_j(t-\tau_j(t))))^* c_{rj}^* + \Sigma_{j=1}^{M}\left(\int_{t-\sigma_{rj}}^{t}\hat{h}_j(e_j(s))ds\right)^* d_{rj}^* \\ &\quad + \rho_{1r}e_r^*(t) - \rho_{2r}((e_r(t))^{\alpha})^* - \rho_{3r}((e_r(t))^{\beta})^* + \rho_{4r}\Sigma_{j=1}^{M}(e_r(t-\tau_{rj}(t)))^* \\ &\quad + \rho_{5r}\Sigma_{j=1}^{M}\left(\int_{t-\sigma_{rj}(t)}^{t}\|e_j(s)\|_1 ds\right)^*\Bigg) sgn(e_r(t)). \end{aligned} \tag{7}$$

$$\begin{aligned} D^+V(t) &= \frac{1}{2}\Sigma_{r=1}^{M}(-a_r + \rho_{1r})\left(sgn(e_r(t))^* e_r(t) + e_r^*(t)sgn(e_r(t))\right) \\ &\quad + \frac{1}{2}\Sigma_{r=1}^{M}\Sigma_{j=1}^{M}\Big(sgn(e_r(t))^* b_{rj}\hat{f}_j(e_j(t)) \\ &\quad + (\hat{f}_j(e_j(t)))^* b_{rj}^* sgn(e_r(t))\Big) + \frac{1}{2}\Sigma_{r=1}^{M}\Sigma_{j=1}^{M}\Big(sgn(e_r(t))^* c_{rj} \\ &\quad \hat{g}_j(e_j(t-\tau_j(t))) + (\hat{g}_j(e_j(t-\tau_j(t))))^* b_{rj}^* \\ &\quad sgn(e_r(t))\Big) + \frac{1}{2}\Sigma_{r=1}^{M}\Sigma_{j=1}^{M}\Bigg(sgn(e_r(t))^* d_{rj}\int_{t-\sigma_{rj}}^{t}\hat{h}_j(e_j(s))ds \\ &\quad + \left(\int_{t-\sigma_{rj}}^{t}\hat{h}_j(e_j(s))ds\right)^* d_{rj}^* sgn(e_r(t))\Bigg) \\ &\quad - \frac{1}{2}\Sigma_{r=1}^{M}\rho_{2r}\Big(sgn(e_r(t))^*(e_r(t))^{\alpha} + ((e_r(t))^{\alpha})^* sgn(e_r(t))\Big) \\ &\quad - \frac{1}{2}\Sigma_{r=1}^{M}\rho_{3r}\Big(sgn(e_r(t))^*(e_r(t))^{\beta} \\ &\quad + ((e_r(t))^{\beta})^* sgn(e_r(t))\Big) + \frac{1}{2}\Sigma_{r=1}^{M}\Sigma_{j=1}^{M}\rho_{4r}\Big(sgn(e_r(t))^* e_r(t-\tau_j(t)) \\ &\quad + e_r^*(t-\tau_j(t))sgn(e_r(t))\Big) \end{aligned}$$

$$+\frac{1}{2}\Sigma_{r=1}^{M}\Sigma_{j=1}^{M}\rho_{5r}\left(sgn(e_r(t))^*\int_{t-\sigma_{rj}(t)}^{t}\|e_j(s)\|_1 ds + \left(\int_{t-\sigma_{rj}(t)}^{t}\|e_j(s)\|_1 ds\right)^* sgn(e_r(t))\right). \quad (8)$$

By using Lemma 2 and Assumption 1, we have

$$\frac{1}{2}\Sigma_{r=1}^{M}(-a_r+\rho_{1r})\left(sgn(e_r(t))^*e_r(t)+e_r^*(t)sgn(e_r(t))\right)$$
$$=\Sigma_{r=1}^{M}(-a_r+\rho_{1r})\|e_r(t)\|_1.$$
$$\frac{1}{2}\Sigma_{r=1}^{M}\Sigma_{j=1}^{M}\left(sgn(e_r(t))^*b_{rj}\hat{f}_j(e_j(t))+(\hat{f}_j(e_j(t)))^*b_{rj}^*sgn(e_r(t))\right)$$
$$\le\Sigma_{r=1}^{M}\Sigma_{j=1}^{M}\|b_{rj}\|_1\|\hat{f}_j(e_j(t))\|_1=\Sigma_{r=1}^{M}\Sigma_{j=1}^{M}\|b_{jr}\|_1F_r\|e_r(t)\|_1. \quad (9)$$
$$\frac{1}{2}\Sigma_{r=1}^{M}\Sigma_{j=1}^{M}\left(sgn(e_r(t))^*c_{rj}\hat{g}_j(e_j(t-\tau_j(t)))+(\hat{g}_j(e_j(t-\tau_j(t))))^*c_{rj}^*sgn(e_r(t))\right)$$
$$+\frac{1}{2}\Sigma_{r=1}^{M}\Sigma_{j=1}^{M}\rho_{4r}\left(sgn(e_r(t))^*e_r(t-\tau_j(t))+e_r^*(t)sgn(e_r(t-\tau_j(t)))^*\right)$$
$$\le\Sigma_{r=1}^{M}\Sigma_{j=1}^{M}\|c_{rj}\|_1\|\hat{g}_j(e_j(t-\tau_j(t)))\|_1+\Sigma_{r=1}^{M}\Sigma_{j=1}^{M}\rho_{4r}\|\hat{g}_j(e_j(t-\tau_j(t)))\|_1$$
$$=\Sigma_{r=1}^{M}\Sigma_{j=1}^{M}\left(\|c_{jr}\|_1G_r+\rho_{4j}G_r\right)\|e_r(t-\tau_r(t))\|_1. \quad (10)$$
$$\frac{1}{2}\Sigma_{r=1}^{M}\Sigma_{j=1}^{M}\left(sgn(e_r(t))^*d_{rj}\int_{t-\sigma_{rj}(t)}^{t}\hat{h}_j(e_j(s))ds + \left(\int_{t-\sigma_{rj}(t)}^{t}\hat{h}_j(e_j(s))ds\right)^* d_{rj}^*sgn(e_r(t))\right)$$
$$+\frac{1}{2}\Sigma_{r=1}^{M}\Sigma_{j=1}^{M}\rho_{5r}\left(sgn(e_r(t))^*\int_{t-\sigma_{rj}(t)}^{t}\|e_j(s)\|_1 ds + \left(\int_{t-\sigma_{rj}(t)}^{t}\|e_j(s)\|_1 ds\right)^* sgn(e_r(t))\right)$$
$$\le\Sigma_{r=1}^{M}\Sigma_{j=1}^{M}\|d_{rj}\|_1\int_{t-\sigma_{rj}(t)}^{t}\|\hat{h}_j(e_j(s))\|_1 ds+\Sigma_{r=1}^{M}\Sigma_{j=1}^{M}\rho_{5r}\int_{t-\sigma_{rj}(t)}^{t}\|e_j(s)\|_1 ds$$
$$\le\Sigma_{r=1}^{M}\Sigma_{j=1}^{M}\left(\|d_{rj}\|_1H_j+\rho_{5r}\right)\int_{t-\sigma_{rj}(t)}^{t}\|e_j(s)\|_1 ds \quad (11)$$
$$-\frac{1}{2}\Sigma_{r=1}^{M}\rho_{2r}\left(sgn(e_r(t))^*(e_r(t))^\alpha+((e_r(t))^\alpha)^*sgn(e_r(t))\right)$$
$$\le-\Sigma_{r=1}^{M}\rho_{2r}\|e_r(t)\|_1^\alpha,\ \text{because } 0<\alpha<1. \quad (12)$$
$$-\frac{1}{2}\Sigma_{r=1}^{M}\rho_{3r}\left(sgn(e_r(t))^*(e_r(t))^\beta+((e_r(t))^\beta)^*sgn(e_r(t))\right)$$
$$\le-M^{1-\beta}\Sigma_{r=1}^{M}\rho_{3r}\|e_r(t)\|_1^\beta,\ \text{because } \beta>1. \quad (13)$$

$$D^+V(t)\le\Sigma_{r=1}^{M}\left(a_r-\rho_{1r}+\Sigma_{j=1}^{M}\|b_{jr}\|_1F_r\right)\|e_r(t)\|_1$$
$$+\Sigma_{r=1}^{M}\Sigma_{j=1}^{M}\left(\|c_{jr}\|_1G_r+\rho_{4j}G_r\right)\|e_r(t-\tau_r(t))\|_1$$
$$-\Sigma_{r=1}^{M}\rho_{2r}\|e_r(t)\|_1^\alpha-M^{1-\beta}\Sigma_{r=1}^{M}\rho_{3r}\|e_r(t)\|_1^\beta$$
$$+\Sigma_{r=1}^{M}\Sigma_{j=1}^{M}\left(\|d_{rj}\|_1H_j+\rho_{5r}\right)\int_{t-\sigma_{rj}(t)}^{t}\|\hat{h}_j(e_j(s))\|_1 ds$$
$$\le-\Sigma_{r=1}^{M}\rho_{2r}\|e_r(t)\|_1^\alpha-M^{1-\beta}\Sigma_{r=1}^{M}\rho_{3r}\|e_r(t)\|_1^\beta$$
$$\le-\rho_2\Sigma_{r=1}^{M}\|e_r(t)\|_1^\alpha-M^{1-\beta}\rho_3\Sigma_{r=1}^{M}\|e_r(t)\|_1^\beta$$
$$\le-\rho_2\left(\Sigma_{r=1}^{M}\|e_r(t)\|_1\right)^\alpha-M^{2(1-\beta)}\rho_3\left(\Sigma_{r=1}^{M}\|e_r(t)\|_1\right)^\beta$$
$$\le-\rho_2\left(V(t)\right)^\alpha-M^{2(1-\beta)}\rho_3\left(V(t)\right)^\beta, \quad (14)$$

where $\rho_2=\min_{1\le r\le M}\{\rho_{2r}\}$, $\rho_3=\min_{1\le r\le M}\{\rho_{3r}\}$.

According to Lemma 3, it can be inferred that the error system (3) exhibits FTS, which means the drive and response systems are synchronized with the controller within a fixed time. Also, one can determine the settling time as $T_1=\frac{1}{\rho_2}\left(\frac{\rho_2}{M^{2(1-\beta)}\rho_3}\right)^{\frac{1-\alpha}{\beta-\alpha}}\left(\frac{1}{\beta-1}+\frac{1}{1-\alpha}\right)$.

This completes the proof of the theorem. □

3.2. FTPS result for master and response systems

The subsequent results are based on projective synchronization, where the synchronization error is characterized as the disparity between the master system and the response system, scaled by a factor. Consequently, the projective synchronization error is defined as

$$e_r(t)=y_r(t)-\delta x_r(t),$$

where δ is the projective coefficient or scaling factor. Subsequently, the projective error equation corresponding to the drive and response systems is expressed as

$$\dot{e}_r(t)=-a_re_r(t)+\Sigma_{j=1}^{M}b_{rj}\left(f_j(y_j(t))-\delta f_j(x_j(t))\right)+\Sigma_{j=1}^{M}c_{rj}\left(g_j(y_j(t-\tau_j(t)))-\delta g_j(x_j(t-\tau_j(t)))\right)+\Sigma_{j=1}^{M}d_{rj}\int_{t-\sigma_{rj}}^{t}\left(h_j(y_j(s))-\delta h_j(x_j(s))\right)ds+U_r(t). \quad (15)$$

Definition 3 ([38]). The master system (1) and the response system (2) are considered FTPS if the error system achieves synchronization within a finite time and the settling time is independent of the initial conditions. An equilibrium point is classified as FTPS if it satisfies the conditions of finite-time stability and, in addition, if the settling time is uniformly bounded, i.e., $T(e_0)<T_{\max}$ for all e_0, where $T_{\max}$ is a constant. Here, the error is defined as the projective error $e_r(t)=y_r(t)-\delta x_r(t)$, where $y_r(t)$ and $x_r(t)$ are response and master system variables and δ is the projection coefficient.

For projective synchronization, the controller needs to be redesigned. For this, let us design the controller as

$$U_r(t)=\xi_re_r(t)-k_{1r}(e_r(t))^\alpha-k_{2r}(e_r(t))^\beta+k_{3r}\int_{t-\sigma_{rj}(t)}^{t}\|e_r(s)\|_1\,ds+k_{4r}e_r(t-\tau_j(t))+\Sigma_{j=1}^{M}b_{rj}\left(\delta f_j(x_j(t))-f_j(\delta x_j(t))\right)+\Sigma_{j=1}^{M}c_{rj}\left(\delta g_j(x_j(t-\tau_j(t)))-g_j(\delta x_j(t-\tau_j(t)))\right)+\Sigma_{j=1}^{M}d_{rj}\int_{t-\sigma_{rj}}^{t}\left(\delta h_j(x_j(s)-h_j(\delta x_j(s))\right)ds. \quad (16)$$

Theorem 2. *Suppose the Assumption 1 holds and if the parameters k_{1r}, k_{2r}, k_{3r} and k_{4r} in the controller satisfy*

$$-a_r+\xi_r+\Sigma_{j=1}^{M}\|b_{jr}\|_1F_r\le0,$$
$$\Sigma_{j=1}^{M}\|c_{jr}\|_1G_r+k_{4r}\le0,$$
$$\Sigma_{j=1}^{M}\|d_{rj}\|_1H_j+k_{3r}\le0,\ k_{1r}>0,\ k_{2r}>0,$$

for $r,j\in I$, then the drive system (1) is projective synchronized with the response system (2) in a fixed time, and the corresponding settling time is estimated as

$$T_2=\frac{1}{k_1}\left(\frac{k_1}{M^{2(1-\beta)}k_2}\right)^{\frac{1-\alpha}{\beta-\alpha}}\left(\frac{1}{\beta-1}+\frac{1}{1-\alpha}\right),$$

where $k_1=\min_{1\le r\le M}\{k_{1r}\}$, $k_2=\min_{1\le r\le M}\{k_{2r}\}$, $0<\alpha<1$ and $\beta>1$.

Proof. Let us construct the Lyapunov function as

$$V(t)=\frac{1}{2}\Sigma_{r=1}^{M}\left(sgn(e_r(t))^*e_r(t)+e_r(t)^*sgn(e_r(t))\right). \quad (17)$$

Differentiate $V(t)$ with respect to t and using the error Eq. (15), we have

$$\begin{aligned}
\dot{V}(t) &= \frac{1}{2}\Sigma_{r=1}^{M}\left(sgn(e_r(t))^*\dot{e}_r(t) + \dot{e}_r(t)^*sgn(e_r(t))\right)\\
&= \frac{1}{2}\Sigma_{r=1}^{M}sgn(e_r(t))^*\Bigg(-a_re_r(t) + \Sigma_{j=1}^{M}b_{rj}\left(f_j(y_j(t)) - \delta f_j(x_j(t))\right)\\
&\quad + \Sigma_{j=1}^{M}c_{rj}\left(g_j(y_j(t-\tau_j(t))) - \delta g_j(x_j(t-\tau_j(t)))\right)\\
&\quad + \Sigma_{j=1}^{M}d_{rj}\int_{t-\sigma_{rj}}^{t}\left(h_j(y_j(s)) - \delta h_j(x_j(s))\right)ds + \xi_re_r(t) - k_{1r}(e_r(t))^{\alpha}\\
&\quad - k_{2r}(e_r(t))^{\beta} + k_{3r}\int_{t-\sigma_{rj}(t)}^{t}\|e_r(s)\|_1 ds + k_{4r}e_r(t-\tau_j(t))\\
&\quad + \Sigma_{j=1}^{M}b_{rj}\left(\delta f_j(x_j(t)) - f_j(\delta x_j(t))\right)\\
&\quad + \Sigma_{j=1}^{M}c_{rj}\left(\delta g_j(x_j(t-\tau_j(t))) - g_j(\delta x_j(t-\tau_j(t)))\right)\\
&\quad + \Sigma_{j=1}^{M}d_{rj}\int_{t-\sigma_{rj}}^{t}\left(\delta h_j(x_j(s)) - h_j(\delta x_j(s))\right)ds\Bigg)\\
&\quad + \frac{1}{2}\Sigma_{r=1}^{M}\Bigg(-a_re_r(t) + \Sigma_{j=1}^{M}b_{rj}\left(f_j(y_j(t)) - \delta f_j(x_j(t))\right)\\
&\quad + \Sigma_{j=1}^{M}c_{rj}\left(g_j(y_j(t-\tau_j(t))) - \delta g_j(x_j(t-\tau_j(t)))\right)\\
&\quad + \Sigma_{j=1}^{M}d_{rj}\int_{t-\sigma_{rj}}^{t}\left(h_j(y_j(s)) - \delta h_j(x_j(s))\right)ds + \xi_re_r(t) - k_{1r}(e_r(t))^{\alpha}\\
&\quad - k_{2r}(e_r(t))^{\beta} + k_{3r}\int_{t-\sigma_{rj}(t)}^{t}\|e_r(s)\|_1 ds + k_{4r}e_r(t-\tau_j(t))\\
&\quad + \Sigma_{j=1}^{M}b_{rj}\left(\delta f_j(x_j(t)) - f_j(\delta x_j(t))\right)\\
&\quad + \Sigma_{j=1}^{M}c_{rj}\left(\delta g_j(x_j(t-\tau_j(t))) - g_j(\delta x_j(t-\tau_j(t)))\right)\\
&\quad + \Sigma_{j=1}^{M}d_{rj}\int_{t-\sigma_{rj}}^{t}\left(\delta h_j(x_j(s)) - h_j(\delta x_j(s))\right)ds\Bigg)^{*}sgn(e_r(t)).
\end{aligned}$$

or,

$$\begin{aligned}
\dot{V}(t) &= \frac{1}{2}\Sigma_{r=1}^{M}sgn(e_r(t))^*\Bigg(-a_re_r(t) + \Sigma_{j=1}^{M}b_{rj}\left(f_j(y_j(t)) - f_j(\delta x_j(t))\right)\\
&\quad + \Sigma_{j=1}^{M}c_{rj}\left(g_j(y_j(t-\tau_j(t))) - g_j(\delta x_j(t-\tau_j(t)))\right)\\
&\quad + \Sigma_{j=1}^{M}d_{rj}\int_{t-\sigma_{rj}}^{t}\left(h_j(y_j(s)) - h_j(\delta x_j(s))\right)ds + \xi_re_r(t) - k_{1r}(e_r(t))^{\alpha}\\
&\quad - k_{2r}(e_r(t))^{\beta} + k_{3r}\int_{t-\sigma_{rj}(t)}^{t}\|e_r(s)\|_1 ds + k_{4r}e_r(t-\tau_j(t))\Bigg)\\
&\quad + \frac{1}{2}\Sigma_{r=1}^{M}\Bigg(-a_re_r^*(t) + \Sigma_{j=1}^{M}\left(f_j(y_j(t)) - f_j(\delta x_j(t))\right)^{*}b_{rj}^*\\
&\quad + \Sigma_{j=1}^{M}\left(g_j(y_j(t-\tau_j(t))) - g_j(\delta x_j(t-\tau_j(t)))\right)^{*}c_{rj}^*\\
&\quad + \Sigma_{j=1}^{M}\left(\int_{t-\sigma_{rj}}^{t}\left(h_j(y_j(s)) - h_j(\delta x_j(s))\right)ds\right)^{*}d_{rj}^*\\
&\quad + \xi_re_r^*(t) - k_{1r}\left((e_r(t))^{\alpha}\right)^{*} - k_{2r}\left((e_r(t))^{\beta}\right)^{*}\\
&\quad + k_{3r}\left(\int_{t-\sigma_{rj}(t)}^{t}\|e_r(s)\|_1 ds\right)^{*} + k_{4r}e_r^*(t-\tau_j(t))\Bigg)sgn(e_r(t)).
\end{aligned}$$

Considering

$\hat{f}_j(e_j(t)) = f_j(y_j(t)) - f_j(\delta x_j(t))$,

$\hat{g}_j(e_j(t)) = g_j(y_j(t)) - g_j(\delta x_j(t))$,

$\hat{h}_j(e_j(t)) = h_j(y_j(t)) - h_j(\delta x_j(t))$ where $j = 1, 2, \ldots, M$,

$$\begin{aligned}
\dot{V}(t) &= \frac{1}{2}\Sigma_{r=1}^{M}(-a_r + \xi r)\left(sgn(e_r(t))^*e_r(t) + e_r^*(t) + sgn(e_r(t))\right)\\
&\quad + \frac{1}{2}\Sigma_{r=1}^{M}\Sigma_{j=1}^{M}\Bigg(sgn(e_r(t))^*b_{rj}\left(f_j(y_j(t))\right.\\
&\quad \left.-f_j(\delta x_j(t))\right) + \left(f_j\left(y_j(t) - f_j(\delta x_j(t)\right)^*b_{rj}^*sgn(e_r(t))\right)\\
&\quad + \frac{1}{2}\Sigma_{r=1}^{M}\Sigma_{j=1}^{M}\left(sgn(e_r(t))^*c_{rj}\left(g_j(y_j(t-\tau_j(t)))\right.\right.\\
&\quad \left.\left.-g_j(\delta x_j(t-\tau_j(t)))\right) + \left(g_j(y_j(t-\tau_j(t)))\right.\right.\\
&\quad \left.\left.-g_j(\delta x_j(t-\tau_j(t)))\right)^*c_{rj}^*sgn(e_r(t))\right)\\
&\quad + \frac{1}{2}\Sigma_{r=1}^{M}\Sigma_{j=1}^{M}\left(sgn(e_r(t))^*d_{rj}\left(\int_{t-\sigma_{rj}}^{t}\left(h_j(y_j(s)) - h_j(\delta x_j(s))\right)ds\right)\right.\\
&\quad \left.+\left(\int_{t-\sigma_{rj}}^{t}\left(h_j(y_j(s))\right.\right.\right.\\
&\quad \left.\left.\left.-h_j(\delta x_j(s))\right)ds\right)^*d_{rj}^*sgn(e_r(t))\right)\\
&\quad - \frac{1}{2}\Sigma_{r=1}^{M}k_{1r}\left(sgn(e_r(t))^*(e_r(t))^{\alpha} + ((e_r(t))^{\alpha})^*sgn(e_r(t))\right)\\
&\quad - \frac{1}{2}\Sigma_{r=1}^{M}k_{2r}\left(sgn(e_r(t))^*(e_r(t))^{\beta} + ((e_r(t))^{\beta})^*sgn(e_r(t))\right)\\
&\quad + \frac{1}{2}\Sigma_{r=1}^{M}k_{4r}\left(sgn(e_r(t))^*e_r(t-\tau_j(t))\right.\\
&\quad \left.+e_r^*(t)sgn(e_r(t-\tau_j(t)))^*\right) + \frac{1}{2}\Sigma_{r=1}^{M}k_{3r}\left(sgn(e_r(t))^*\int_{t-\sigma_{rj}(t)}^{t}\|e_j(s)\|_1 ds\right.\\
&\quad \left.+\left(\int_{t-\sigma_{rj}(t)}^{t}\|e_j(s)\|_1 ds\right)^*sgn(e_r(t))\right). \qquad (18)
\end{aligned}$$

By Lemma 1 and Assumption 1, we have

$$\begin{aligned}
&\frac{1}{2}\Sigma_{r=1}^{M}(-a_r + \xi_r)\left(sgn(e_r(t))^*e_r(t) + e_r^*(t)sgn(e_r(t))\right)\\
&\quad = \Sigma_{r=1}^{M}(-a_r + \xi_r)\|e_r(t)\|_1. \qquad (19)\\
&\frac{1}{2}\Sigma_{r=1}^{M}\Sigma_{j=1}^{M}\Bigg(sgn(e_r(t))^*b_{rj}\left(f_j(y_j(t)) - f_j(\delta x_j(t))\right)\\
&\quad + \left(f_j(y_j(t) - f_j(\delta x_j(t))\right)^*b_{rj}^*sgn(e_r(t))\Bigg)\\
&\quad \le \Sigma_{r=1}^{M}\Sigma_{j=1}^{M}\|b_{rj}\|_1\|\left(f_j(y_j(t)) - f_j(\delta x_j(t))\right)\|_1\\
&\quad \le \Sigma_{r=1}^{M}\Sigma_{j=1}^{M}\|b_{rj}\|_1F_j\|e_j(t)\|_1 = \Sigma_{r=1}^{M}\Sigma_{j=1}^{M}\|b_{jr}\|_1F_r\|e_r(t)\|_1. \qquad (20)\\
&\frac{1}{2}\Sigma_{r=1}^{M}\Sigma_{j=1}^{M}\Bigg(sgn(e_r(t))^*c_{rj}\left(g_j(y_j(t-\tau_j(t))) - g_j(\delta x_j(t-\tau_j(t)))\right)\\
&\quad + \left(g_j(y_j(t-\tau_j(t))) - g_j(\delta x_j(t-\tau_j(t)))\right)^*c_{rj}^*sgn(e_r(t))\Bigg)\\
&\quad + \frac{1}{2}\Sigma_{r=1}^{M}k_{4r}\left(sgn(e_r(t))^*e_r(t-\tau_j(t)) + e_r^*(t)sgn(e_r(t-\tau_j(t)))^*\right)\\
&\quad \le \Sigma_{r=1}^{M}\Sigma_{j=1}^{M}\|c_{rj}\|_1\|\left(g_j(y_j(t-\tau_j(t))) - g_j(\delta x_j(t-\tau_j(t)))\right)\|_1\\
&\quad + \Sigma_{r=1}^{M}\Sigma_{j=1}^{M}k_{4r}\|e_j(t-\tau_j(t))\|_1\\
&\quad \le \Sigma_{r=1}^{M}\Sigma_{j=1}^{M}\left(\|c_{rj}\|_1G_j + k_{4r}\right)\|e_j(t-\tau_j(t))\|_1\\
&\quad = \Sigma_{r=1}^{M}\Sigma_{j=1}^{M}\left(\|c_{jr}\|_1G_r + k_{4j}\right)\|e_r(t-\tau_r(t))\|_1. \qquad (21)\\
&\frac{1}{2}\Sigma_{r=1}^{M}\Sigma_{j=1}^{M}\Bigg(sgn(e_r(t))^*d_{rj}\left(\int_{t-\sigma_{rj}}^{t}\left(h_j(y_j(s)) - h_j(\delta x_j(s))\right)ds\right)\\
&\quad + \left(\int_{t-\sigma_{rj}}^{t}\left(h_j(y_j(s)) - h_j(\delta x_j(s))\right)ds\right)^*d_{rj}^*sgn(e_r(t))\Bigg)\\
&\quad + \frac{1}{2}\Sigma_{r=1}^{M}k_{3r}\left(sgn(e_r(t))^*\int_{t-\sigma_{rj}(t)}^{t}\|e_j(s)\|_1 ds\right.\\
&\quad \left.+\left(\int_{t-\sigma_{rj}(t)}^{t}\|e_j(s)\|_1 ds\right)^*sgn(e_r(t))\right)\\
&\le \Sigma_{r=1}^{M}\Sigma_{j=1}^{M}\|d_{rj}\|_1\int_{t-\sigma_{rj}(t)}^{t}\int_{t-\sigma_{rj}(t)}^{t}\|h_j(y_j(s)) - h_j(\delta x_j(s))\|_1 ds\\
&\quad + \Sigma_{r=1}^{M}\Sigma_{j=1}^{M}k_{3r}\int_{t-\sigma_{rj}(t)}^{t}\|e_j(s)\|_1 ds
\end{aligned}$$

$$\leq \Sigma_{r=1}^{M}\Sigma_{j=1}^{M}\left(\|d_{jr}\|_1 H_j + k_{3r}\right)\int_{t-\sigma_{rj}(t)}^{t}\|e_j(s)\|_1 ds$$

$$= \Sigma_{r=1}^{M}\Sigma_{j=1}^{M}\left(\|d_{rj}\|_1 H_r + k_{3r}\right)\int_{t-\sigma_{rj}(t)}^{t}\|e_r(s)\|_1 ds. \quad (22)$$

$$-\frac{1}{2}\Sigma_{r=1}^{M}k_{1r}\left(sgn(e_r(t))^*(e_r(t))^{\alpha} + ((e_r(t))^{\alpha})^* sgn(e_r(t))\right)$$

$$\leq -\Sigma_{r=1}^{M}k_{1r}\|e_r(t)\|_1^{\alpha}, \text{since } 0<\alpha<1. \quad (23)$$

$$-\frac{1}{2}\Sigma_{r=1}^{M}k_{2r}\left(sgn(e_r(t))^*(e_r(t))^{\beta} + ((e_r(t))^{\beta})^* sgnk_{2r}\|e_r(t)\|_1^{\beta}, \text{since } \beta>1. \quad (24)$$

From the Eqs. (19)–(24) in the Eq. (18), we have

$$\dot{V}(t) \leq \Sigma_{r=1}^{M}\left(-a_r + \xi_r + \Sigma_{j=1}^{M}\|b_{jr}\|_1 F_r\right)\|e_r(t)\|_1$$
$$+\Sigma_{r=1}^{M}\Sigma_{j=1}^{M}\left(\|c_{jr}\|_1 G_r + k_{4j}\right)\|e_r(t-\tau_r(t))\|_1$$
$$-\Sigma_{r=1}^{M}k_{1r}\|e_r(t)\|_1^{\alpha} - M^{1-\beta}\Sigma_{r=1}^{M}k_{2r}\|e_r(t)\|_1^{\beta} + \Sigma_{r=1}^{M}\Sigma_{j=1}^{M}\left(\|d_{rj}\|_1 H_j + k_{3r}\right)$$
$$\int_{t-\sigma_{rj}(t)}^{t}\|\hat{h}_j(e_j(s))\|_1 ds$$
$$\leq -\Sigma_{r=1}^{M}k_{1r}\|e_r(t)\|_1^{\alpha} - M^{1-\beta}\Sigma_{r=1}^{M}k_{2r}\|e_r(t)\|_1^{\beta}$$
$$\leq -k_1\Sigma_{r=1}^{M}\|e_r(t)\|_1^{\alpha} - M^{1-\beta}k_2\Sigma_{r=1}^{M}\|e_r(t)\|_1^{\beta}$$
$$\leq -k_1\left(\Sigma_{r=1}^{M}\|e_r(t)\|_1\right)^{\alpha} - M^{2(1-\alpha)}k_2\left(\Sigma_{r=1}^{M}\|e_r(t)\|_1\right)^{\beta}.$$

or,

$$\dot{V}(t) \leq -k_1\left(V(t)\right)^{\alpha} - M^{2(1-\beta)}k_2\left(V(t)\right)^{\beta}, \quad (25)$$
$$\text{where } k_1 = \min_{1\leq r\leq M}\{k_{1r}\},\ k_2 = \min_{1\leq r\leq M}\{k_{2r}\},\ 0<\alpha<1 \text{ and } \beta>1.$$

Based on Lemma 3, it follows that the error system is projectively fixed-time synchronized, i.e., the drive system (1) and response system (2) achieve synchronization in a fixed time with the controller (16).

Furthermore, one can estimate the setting time by the following equality: $T_2 = \frac{1}{k_1}\left(\frac{k_1}{M^{2(1-\beta)}k_2}\right)^{\frac{1-\alpha}{\beta-\alpha}}\left(\frac{1}{\beta-1}+\frac{1}{1-\alpha}\right)$.

The proof is completed. □

Remark 6. When exploring the dynamical characteristics of QVNNs and OVNNs, the researchers have considered several approaches to address the challenges posed by non-commutative and non-associative octonion multiplication, including decomposition [24,28,50] and linear matrix inequality [51]. However, in this article, a non-decomposition method has achieved the FTS and FTPS of a specific type of OVNNs with mixed delay. To the best of our knowledge, this type of research work has yet to be done in this area, and it significantly reduces the computational complexity in the study of OVNNs.

Remark 7. The analysis of Theorems 1 and 2 underscores the utility and broad acceptance of the enhanced one-norm approach for octonions. In contrast to the decomposition method proposed in [50], which requires four Lyapunov analyses, our proposed method simplifies the theoretical derivation by necessitating only one Lyapunov analysis. Consequently, our approach is more concise as compared to [24,28,50]. Moreover, our method allows for non-decomposed activation functions, making it less conservative and providing effective results.

Remark 8. The projective error is defined as

$$e_r(t) = y_r(t) - \delta x_r(t),$$

where the factor δ is the scaling factor or projective coefficient. One can deduce several types of synchronization within the fixed-time framework. If we choose $\delta = 1$, then it becomes the error defined in Theorem 1. Again, the proposed results correspond to the anti-synchronization case if one selects the projective coefficient $\delta = -1$. The results obtained for the quaternion domain are special cases, as seen in [23,52,53]. However, to date, there are no such results for OVNNs.

Remark 9. The proposed model (1) serves as a generalization of several lower-dimensional neural network models, depending on the nature of its coefficient weight matrices b_{rj}, c_{rj}, and d_{rj}, as well as the activation functions.

When these coefficient matrices and activation functions belong to the set of real numbers and $d_{rj} = 0$, the model corresponds to the real-valued frameworks discussed in [54–56]. Furthermore, if both $c_{rj} = 0$ and $d_{rj} = 0$, it reduces to the classical real-valued neural network model presented in [57]. In the case where the coefficients are complex-valued and $d_{rj} = 0$, the model becomes equivalent to the complex-valued models studied in [58,59]. Setting $c_{rj} = 0$ and $d_{rj} = 0$ further simplifies the model to the delay-free complex-valued model reported in [60]. For quaternion-valued coefficient matrices and activation functions, the absence of distributed delay ($d_{rj} = 0$) yields a model equivalent to that described in [61]. Additionally, setting both $c_{rj} = 0$ and $d_{rj} = 0$ leads to the form analyzed in [50]. Finally, when the coefficients lie in the octonion domain and $d_{rj} = 0$, the model aligns with the octonion-valued frameworks proposed in [62,63]. Further setting $c_{rj} = 0$ reduces it to a delay-free structure similar to that in [57]. Thus, by suitable choices of the weight connection matrices and activation functions, the proposed model can describe several classes of neural network models, and the derived criteria for various dynamical properties can be directly applied to these specific cases.

Remark 10. The controllers presented in this paper are fundamentally different from those designed in [24,50,61,64–66]. Unlike [24], which employs a discontinuous signum-based controller in the quaternion domain, the proposed design avoids discontinuities, thereby eliminating chattering and enhancing feasibility for real-time implementation. In contrast, to [61,64], which omit distributed delay terms, the current controller incorporates integral components of the form $\int_{t-\sigma_{rj}(t)}^{t}\|e_j(s)\|_1 ds$, allowing for more accurate modeling of memory-dependent dynamics. The work [50] excludes both discrete and distributed delays, further underscoring the novelty of our delay-aware control approach. While [65] introduces two separate controllers using switching strategies; the present work proposes a unified control structure that achieves fixed-time synchronization without switching. Compared to [66], which relies entirely on nonlinear terms, including sigma functions, the proposed controller integrates both linear and nonlinear components. This hybrid structure balances robustness with analytical tractability: the linear terms ensure system stability, while the nonlinear terms, specifically $e_r(t)^{\alpha}$ and $e_r(t)^{\beta}$, accelerate convergence and guarantee synchronization within a fixed time. Overall, the proposed controller significantly generalizes prior fixed-time synchronization results by explicitly incorporating discrete and distributed delays—unlike earlier QVNN studies such as [24,61]. This leads to enhanced performance, more accurate modeling, and broader applicability to complex delayed neural systems.

Remark 11. Extensive research has been conducted on the synchronization of OVNNs and QVNNs, as evidenced by [24,28–30,49,61,62,65]. Notably, the FTS of OVNNs has been studied in [28,49,62]. However, the decomposition method proposed in [28] is relatively complex. These existing methods increase computational complexity because they require decomposing both the original system and the controller, resulting in multiple separate conditions instead of a unified criterion. Moreover, it necessitates four or more Lyapunov analyses, further complicating the theoretical derivations. In the present study, we propose a non-decomposition method to investigate the synchronization of OVNNs. By employing an improved one-norm of the octonion, we design octonion-valued controllers directly, thereby eliminating the need for complex decomposition and extending the existing results in the octonion domain. Our approach requires only a single Lyapunov

Algorithm 1 Synchronization algorithm for delayed neural networks.

Input: Initial states $x_r(0), y_r(0) \in \mathbb{O}$;
System parameters $\alpha_r, \beta_r, a_r, b_{rj}, c_{rj}, d_{rj}$;
Delays $\tau_{rj}(t), \sigma_{rj}(t)$; impulse times $\{t_p\}$
Output: Synchronization behaviour: $\|x_r(t) - y_r(t)\| \to 0$
Step 1: Define the drive-response systems

$$\dot{x}_r(t) = F_r\left(x(t), x(t-\tau_{rj}(t)), \int h(x(\theta))\, d\theta\right)$$

$$\dot{y}_r(t) = F_r\left(y(t), y(t-\tau_{rj}(t)), \int h(y(\theta))\, d\theta\right) + U_r(t)$$

Step 2: Construct synchronization error
Define the error: $e_r(t) = y_r(t) - \delta x_r(t)$
For $\delta = 1$, the error for Theorem 1; and for $\delta > 0$, the error for Theorem 2.
Step 3: Design control input
Choose $U_r(t)$ such that:

$\dot{e}_r(t) =$ dynamics governed by delays, impulses, and $U_r(t)$

Step 4: Construct Lyapunov candidate function
Define a Lyapunov function $V(t)$ positive definite in $e(t), \dot{e}(t)$
Step 5: Derive synchronization condition

$$\dot{V}(t) \le -aV^{\alpha}(e(t)) - bV^{\beta}(e(t)), \quad a, b > 0,\ 0 < \alpha < 1,\ \beta > 1$$

Step 6: Verification via DDE Solver
Simulate the systems using a DDE solver in MATLAB to validate results
Step 7: Verify convergence, Check and Synchronization Conclusion

$$\lim_{t \to T} \|e_r(t)\| = 0$$

Return: System is synchronized if $\|e_r(t)\| \to 0$ as $t \to T$

analysis, making it significantly more concise than the method in [28]. Additionally, it accommodates non-decomposable activation functions, rendering the derived conditions less conservative and enhancing the applicability of the results.

The proposed Algorithm 1 begins by initializing the initial conditions and time delays, along with specifying the drive and response systems. The detailed steps of the algorithm for achieving synchronization are outlined below. By following these steps systematically, we obtain the desired synchronization results.

4. Numerical examples

This study retests suitable parametric values and activation functions to ensure that the theorem conditions are easily satisfied.

Example 1. In order to verify our proposed FTS results, let us consider the two-dimensional OVNNs in the master system as

$$\dot{x}_r(t) = -a_r x_r(t) + \Sigma_{j=1}^{M} b_{rj} f_j(x_j(t)) + \Sigma_{j=1}^{M} c_{rj} g_j(x_j(t-\tau_{rj}(t))) + \Sigma_{j=1}^{M} d_{rj} \int_{t-\sigma_{rj}(t)}^{t} h_j(x_j(s)) ds, \tag{26}$$

and the corresponding response system is

$$\dot{y}_r(t) = -a_r y_r(t) + \Sigma_{j=1}^{M} b_{rj} f_j(y_j(t)) + \Sigma_{j=1}^{M} c_{rj} g_j(y_j(t-\tau_{rj}(t))) + \Sigma_{j=1}^{M} d_{rj} \int_{t-\sigma_{rj}(t)}^{t} h_j(y_j(s)) ds + U_r(t), \tag{27}$$

where $r, j = 1, 2$, $M = 2$ and let us consider the parametric values for the proposed models (26) and (27) as $a_r = 1, \rho_{11} = -30, \rho_{12} = -40, \rho_{21} = 4, \rho_{22} = 3, \rho_{31} = 10, \rho_{32} = 30, \rho_{41} = -38, \rho_{42} = -45, \rho_{51} = -40, \rho_{52} = -46, \alpha = 0.5, \beta = 1.05$.

$$\begin{aligned}
b_{11} &= w_0 - w_1 + 0.5w_2 + 0.9w_3 + 2w_4 + 0.2w_5 - 0.5w_6 + 1.3w_7,\\
b_{12} &= 0.7w_0 + w_1 - 1.3w_2 + 0.2w_3 - w_4 - 1.5w_5 + 0.3w_6 - 1.2w_7,\\
b_{21} &= -w_0 + 1.1w_1 - 0.4w_2 - 0.6w_3 + w_4 + 1.3w_5 + w_6 - 0.6w_7,\\
b_{22} &= 0.8w_0 - 0.7w_1 + 0.8w_2 - 0.5w_3 + 0.8w_4 + 1.2w_5 - 0.6w_6 + 0.5w_7,\\
c_{11} &= w_0 - 0.9w_1 + 2.1w_2 + w_3 + w_4 - 0.9w_5 - 1.1w_6 + w_7,\\
c_{12} &= 0.9w_0 - 2w_1 - w_2 - 1.2w_3 + 2w_4 + 1.4w_5 - w_6 + 1.1w_7,\\
c_{21} &= 1.3w_0 - w_1 - 0.5w_2 - 1.5w_3 + 0.9w_4 - w_5 + 0.4w_6 + 0.4w_7,\\
c_{22} &= 0.6w_0 - 0.9w_1 + 1.4w_2 - 1.4w_3 + 1.2w_4 - w_5 + 1.4w_6 + 0.7w_7,\\
d_{11} &= 1.2w_0 - 0.2w_1 + 1.1w_2 - 0.6w_3 + w_4 - 0.7w_5 + 1.1w_6 - w_7,\\
d_{12} &= 2w_0 + 2w_1 - w_2 + 1.1w_3 + 2w_4 + 2w_5 - w_6 + 1.1w_7,\\
d_{21} &= w_0 - w_1 + 0.4w_2 + 0.6w_3 + 3w_4 - w_5 + 0.4w_6 + 0.6w_7,\\
d_{22} &= 0.2w_0 - w_1 + 2w_2 + 1w_3 + 0.2w_4 - w_5 + 2w_6 + w_7.
\end{aligned}$$

The activation function is considered as $f(.) = g(.) = h(.) = \tanh\left(z^0(t)\right) w_0 + \tanh\left(z^1(t)\right) w_1 + \tanh\left(z^2(t)\right) w_2 + \cdots + \tanh\left(z^7(t)\right) w_7$.The initial values of systems are

$$\begin{aligned}
x_1(0) &= -0.5 + 1.4w_1 + 1.0w_2 + 0.3w_3 - 2.0w_4 + 1.1w_5 + 0.1w_6 + 0.9w_7,\\
x_2(0) &= -0.5 + 0.6w_1 - 0.5w_2 - 0.1w_3 + 0.3w_4 + 0.8w_5 + 0.5w_6 + 0.1w_7,\\
y_1(0) &= -1 + 1.5w_1 + 0.3w_2 + 0.5w_3 - 0.6w_4 - 0.9w_5 + 0.4w_6 + 0.5w_7,\\
y_2(0) &= 0.5 + 0.5w_1 - 0.1w_2 + 0.2w_3 + 0.4w_4 + 0.6w_5 + 0.2w_6 - 0.5w_7.
\end{aligned}$$

For these parametric values and the functions all the conditions of the Theorem 1 are satisfied and the corresponding estimated settling time expression is:

$$T_1 = \frac{1}{\rho_2}\left(\frac{\rho_2}{M^{2(1-\beta)}\rho_3}\right)^{\frac{1-\alpha}{\beta-\alpha}}\left(\frac{1}{\beta-1} + \frac{1}{1-\alpha}\right),$$

where $\rho_2 = \min\{\rho_{21}, \rho_{22}\} = \min\{4, 3\} = 2,\ M = 2$

and $\rho_3 = \min\{\rho_{31}, \rho_{32}\} = \min\{10, 30\} = 10$ then $T_1 = 2.6141$.

The controller function for $r = 1$ is

$$U_1(t) = -30e_1(t) - 4(e_1(t))^{0.5} - 10(e_1(t))^{1.05} - 38\Sigma_{j=1}^{2} e_1(t - \cos^2(t)) - 40\Sigma_{j=1}^{2} \int_{t-\cos^2(t)}^{t} \|e_1(s)\|_1 ds. \tag{28}$$

Again, for $r = 2$, the second controller function becomes

$$U_2(t) = -40e_2(t) - 3(e_2(t))^{0.5} - 30(e_2(t))^{1.05} - 45\Sigma_{j=1}^{2} e_2(t - \cos^2(t)) - 46\Sigma_{j=1}^{2} \int_{t-\cos^2(t)}^{t} \|e_2(s)\|_1 ds. \tag{29}$$

From this, it is observed that the drive and response systems (26) and (27) are synchronized with each other, which are depicted through Figs. 1–4. The corresponding error with controllers is depicted through Figs. 5 and 6, and it is observed from the error graphs that systems reach their desired target within the fixed time.

Remark 12. The settling time T_1 is not only governed by the design parameters α and β, but also exhibits strong sensitivity to the control gain parameters ρ_{2r} and ρ_{3r}. For instance, when $\alpha = 0.5$ and $\beta = 2$, the desired settling time $T_1 = 2.6$ is achieved using control gains $\rho_{21} = 2$, $\rho_{22} = 1$, $\rho_{31} = 10$, and $\rho_{32} = 6$. However, for the same value of $\alpha = 0.5$ but a larger $\beta = 2.6$, the same settling time can be maintained by appropriately adjusting the gains to $\rho_{21} = 2$, $\rho_{22} = 3$, $\rho_{31} = 1$, and $\rho_{32} = 3$.

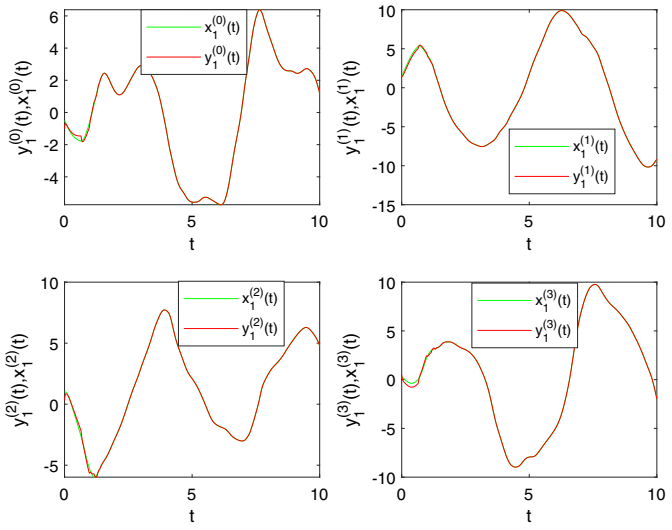

Fig. 1. The trajectories of the first four components of the drive and response systems (26), (27) with controller (28).

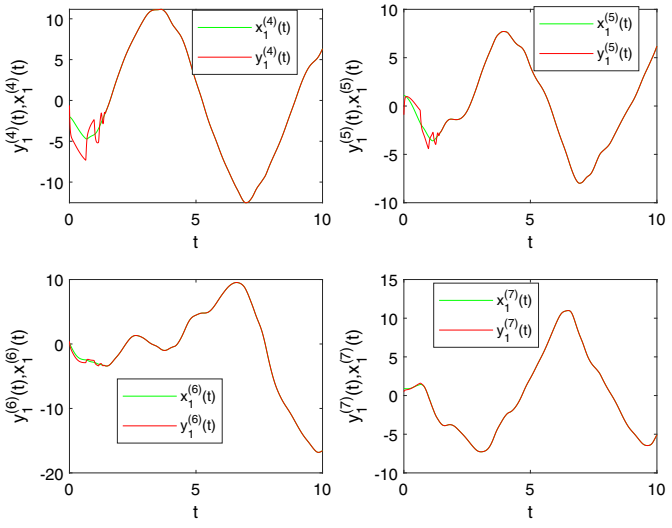

Fig. 2. The trajectories of the last four components of the drive and response systems (26), (27) with controller (28).

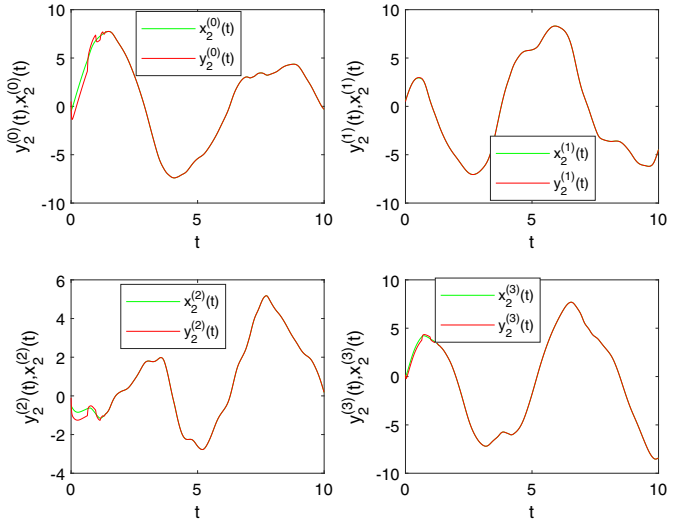

Fig. 3. The trajectories of the first four components of the drive and response systems (26), (27) with controller (29).

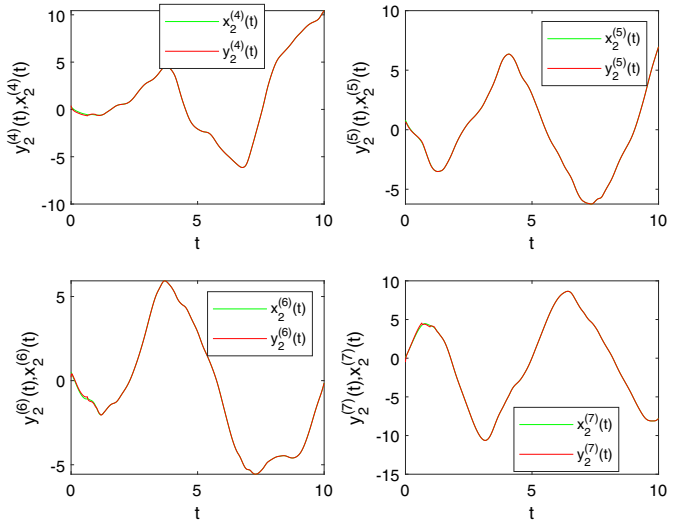

Fig. 4. The trajectories of the last four components of the drive and response systems (26), (27) with controller (29).

This observation underscores the importance of carefully tuning these parameters, as they play a pivotal role in regulating the convergence behaviour of the system.

Remark 13. The computed settling time for Example 1, obtained using Lemma 3, is $T_1 = 2.6141$. In contrast, applying the Lemma referenced in Remark 5 to the same problem results in a longer settling time of $\hat{T}_1 = 2.8102$. This demonstrates the advantage of Lemma 3, which yields a more accurate and tighter estimate of the convergence time. The comparison provides strong computational support for the claim made in Remark 5, confirming that the analytical results derived via Lemma 3 are theoretically more precise and practically more efficient than those based on the Lemma mentioned in Remark 5.

Remark 14. The settling time for the proposed model is $T_1 = 2.6141$ for OVNNs with mixed delays, which is substantially lower than the settling time $\hat{T}^O_{\text{set}} = 2.9641$ reported for OVNNs with time-varying delays (see [28]) with the same parameters considered in our case. It is also lower than the result for QVNNs, $\hat{T}^Q_{\text{set}} = 2.8858$, in [67] (without time-varying delays), and the fixed-time complex-valued neural network result, $\hat{T}^C_{\text{set}} = 2.666$, in [59]. These findings demonstrate that the proposed control strategy achieves faster convergence than conventional approaches, confirming its effectiveness across different algebraic frameworks. Moreover, whereas existing results typically rely on separation or decomposition methods, we adopt a non-separation approach, significantly reducing the derived results' computational burden.

Remark 15. Comparison of our considered controller based on ℓ_1-norm with the other controller based on ℓ_2-norm.

Let us consider the ℓ_1-norm controllers defined in Eqs. (28) and (29), and the ℓ_2-norm controllers defined as follows.

For $r = 1$, the controller is given by:

$$U_1^*(t) = -30e_r(t) - 4(e_r(t))^{0.5} - 10(e_r(t))^{1.05} - 38\Sigma_{j=1}^2 e_r(t - \cos^2(t)) - 40\Sigma_{j=1}^2 \int_{t-\cos^2(t)}^{t} \|e_r(s)\|_1 \, ds. \tag{30}$$

The parameters used in controller (30) are the same as those in Example 1. The derivative of the associated Lyapunov function is

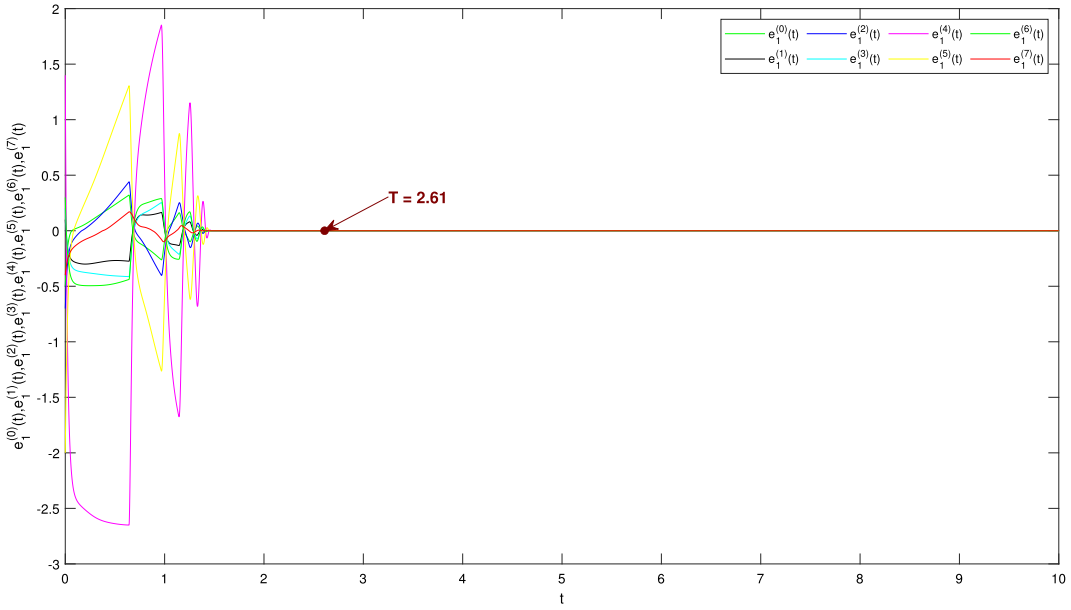

Fig. 5. The Error trajectories of all the components of the drive and response systems (26), (27) with controller (28) for $r = 1$.

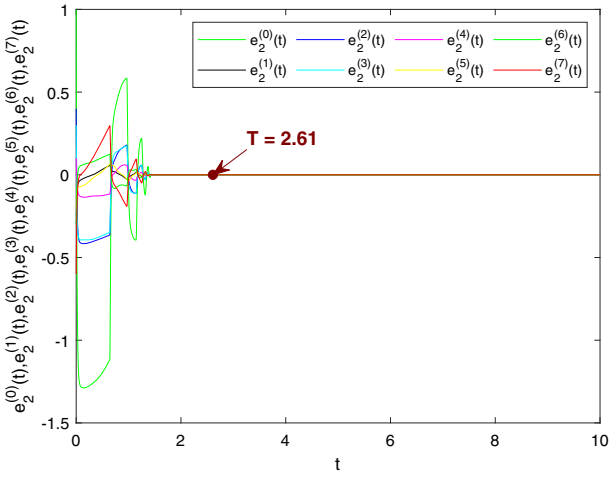

Fig. 6. The Error trajectories of all the components of the drive and response systems (26), (27) with controller (29) for $r = 2$.

expressed as:

$$D^{+}V(t) \le -q\big(V(t)\big)^{\delta} - p\big(V(t)\big)^{\lambda}, \quad p, q > 0, \quad 0 < \delta < 1, \quad \lambda > 1. \tag{31}$$

The settling time is calculated by

$$T_1^* = \frac{1}{q}\left(\frac{q}{p}\right)^{\frac{1-\delta}{\lambda-\delta}}\left(\frac{1}{\lambda-1}+\frac{1}{1-\delta}\right), \text{ where } p = \min_{1\le r\le M}\left\{\rho_{2r} M^{\frac{1-\beta}{2}} 2^{\frac{3-\beta}{2}}\right\},$$
$$q = \min_{1\le r\le M}\left\{2\rho_{3r}\right\}, \delta = \frac{1+\alpha}{2}, \lambda = \frac{1+\beta}{2}$$

It is evident that for $0 < \alpha < 1$ and $\beta > 1$, the conditions $0 < \delta < 1$ and $\lambda > 1$ are satisfied. For the numerical simulations, we adopt the specific parameter values: $p = 5.8$, $q = 20$, $\delta = 0.75$, and $\lambda = 1.025$, while all other parameters remain consistent with those presented in Example 1.

Under the controller defined in equation (30), the observed settling time is $T_1^* = 6.77$. It is clearly observed that $T_1^* > T_1$ under identical parameter settings, indicating that the settling time achieved by the controllers (28) and (29), which employ the ℓ_1-norm, is more efficient and precise than that obtained by the ℓ_2-norm-based controller (30) under the same conditions.

Example 2. In order to verify our proposed FTPS result, let us consider the two-dimensional OVNNs as the master and response systems as

$$\dot{x}_r(t) = -a_r x_r(t) + \Sigma_{j=1}^{M} b_{rj} f_j(x_j(t)) + \Sigma_{j=1}^{M} c_{rj} g_j(x_j(t-\tau_{rj}(t))) + \Sigma_{j=1}^{M} d_{rj} \int_{t-\sigma_{rj}(t)}^{t} h_j(x_j(s))ds, \tag{32}$$

and the corresponding response system is

$$\dot{y}_r(t) = -a_r y_r(t) + \Sigma_{j=1}^{M} b_{rj} f_j(y_j(t)) + \Sigma_{j=1}^{M} c_{rj} g_j(y_j(t-\tau_{rj}(t))) + \Sigma_{j=1}^{M} d_{rj} \int_{t-\sigma_{rj}(t)}^{t} h_j(y_j(s))ds + U_r(t), \tag{33}$$

where $r, j = 1, 2, M = 2$. The corresponding controller is designed as:

$$\begin{aligned} U_r(t) = {} & \xi_r e_r(t) - k_{1r}(e_r(t))^{\alpha} - k_{2r}(e_r(t))^{\beta} + k_{3r}\int_{t-\sigma_{rj}(t)}^{t} \|e_r(s)\|_1 \, ds \\ & + k_{4r} e_r(t-\tau_j(t)) + \Sigma_{j=1}^{M} b_{rj}\big(\delta f_j(x_j(t)) \\ & - f_j(\delta x_j(t))\big) + \Sigma_{j=1}^{M} c_{rj}\big(\delta g_j(x_j(t-\tau_j(t))) - g_j(\delta x_j(t-\tau_j(t)))\big) \\ & + \Sigma_{j=1}^{M} d_{rj}\int_{t-\sigma_{rj}}^{t}\big(\delta h_j(x_j(s) - h_j(\delta x_j(s))\big)ds. \end{aligned} \tag{34}$$

Let us consider the parametric values for the models (32) and (33) and the controller (34) are as below $a_r = 2, \xi_r = 35, k_{11} = 11, k_{12} = 10, k_{21} = 6, k_{22} = 9, k_{31} = -20, k_{32} = -30, k_{41} = -38, k_{42} = -45, \alpha = 0.5, \beta = 1.1, \delta = 0.4$,

$$\begin{aligned} b_{11} &= -w_0 - 0.2w_1 + 0.3w_2 - 1.1w_3 + 1.5w_4 + 0.5w_5 - 0.6w_6 - 0.3w_7, \\ b_{12} &= -0.4w_0 + 0.1w_1 + 1.1w_2 + 0.4w_3 - 0.6w_4 - 1.3w_5 - 0.7w_6 - 1.2w_7, \\ b_{21} &= 0.7w_0 + 1.2w_1 + 0.7w_2 - 1.3w_3 - w_4 + 1.1w_5 - w_6 - 0.3w_7, \\ b_{22} &= -0.4w_0 - 0.3w_1 - 1.8w_2 - 0.5w_3 + 0.8w_4 - 1.1w_5 - 0.6w_6 - 1w_7, \\ c_{11} &= -w_0 - 0.4w_1 + 1.1w_2 - 0.5w_3 + w_4 + 0.9w_5 + 1.1w_6 - 0.1w_7, \\ c_{12} &= 0.25w_0 + 1.8w_1 + w_2 - 1.5w_3 - 0.4w_4 - 1.4w_5 - w_6 + 1.2w_7, \end{aligned}$$

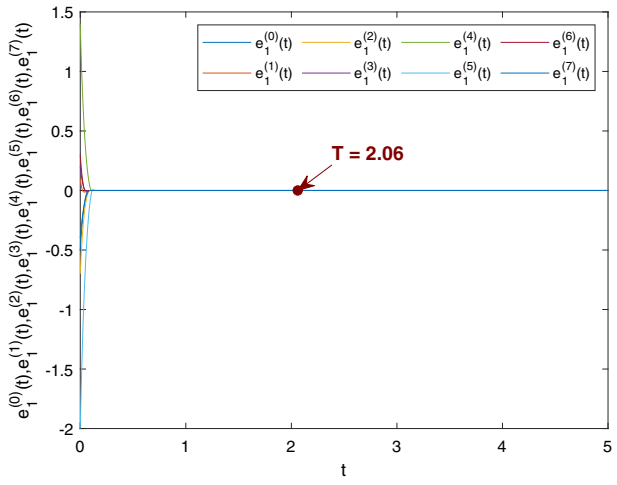

Fig. 7. The Error trajectories of all the components of the drive and response systems (32), (33) with controller (34) for $r = 1$.

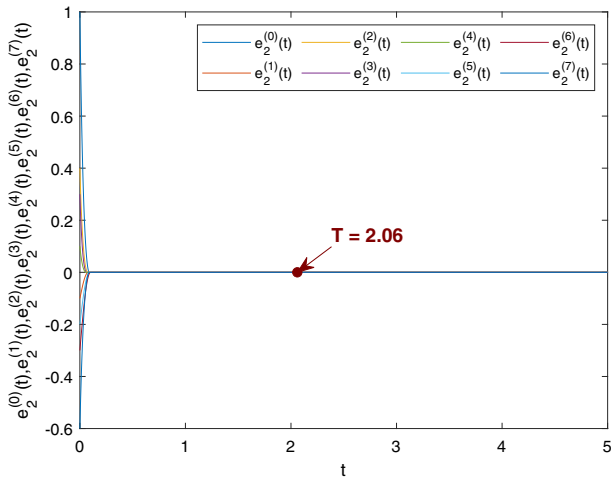

Fig. 8. The Error trajectories of all the components of the drive and response systems (32), (33) with controller (34) for $r = 2$.

$$c_{21} = 1.3w_0 - w_1 - 0.5w_2 - 1.5w_3 + 0.9w_4 - w_5 + 0.4w_6 + 0.4w_7,$$

$$c_{22} = 0.6w_0 - 0.9w_1 + 1.4w_2 - 1.1w_3 + 1.5w_4 - w_5 - 1.6w_6 + 0.7w_7,$$

$$d_{11} = -1.2w_0 - 0.2w_1 - 1.4w_2 - 0.6w_3 + w_4 - 0.7w_5 + 1.1w_6 - w_7,$$

$$d_{12} = -2w_0 + 2w_1 - w_2 - 1.3w_3 + 2w_4 + 2w_5 - w_6 + 1.1w_7,$$

$$d_{21} = w_0 - w_1 + 0.4w_2 + 0.1w_3 + 3w_4 - w_5 - 0.7w_6 + 0.6w_7,$$

$$d_{22} = -0.7w_0 - w_1 + 2w_2 + 1w_3 + 0.2w_4 - w_5 + 2w_6 + w_7.$$

with $\tau_{rj}(t) = \sin^2(t), \sigma_{rj} = \sin^2(t)$, The activation function is given as $f(.) = g(.) = h(.) = \tanh\left(z^0(t)\right) w_0 + \tanh\left(z^1(t)\right) w_1 + \tanh\left(z^2(t)\right) w_2 + \cdots + \tanh\left(z^7(t)\right) w_7$. The initial values of systems are

$$x_1(0) = -0.5 + 1.4w_1 + 1.0w_2 + 0.3w_3 - 2.0w_4 + 1.1w_5 + 0.1w_6 + 0.9w_7,$$

$$x_2(0) = -0.5 + 0.6w_1 - 0.5w_2 - 0.1w_3 + 0.3w_4 + 0.8w_5 + 0.5w_6 + 0.1w_7,$$

$$y_1(0) = -1 + 1.5w_1 + 0.3w_2 + 0.5w_3 - 0.6w_4 - 0.9w_5 + 0.4w_6 + 0.5w_7,$$

$$y_2(0) = 0.5 + 0.5w_1 - 0.1w_2 + 0.2w_3 + 0.4w_4 + 0.6w_5 + 0.2w_6 - 0.5w_7.$$

For these parametric values and the functions, all the conditions of Theorem 2 are satisfied, and the settling time is calculated by:

$$T_2 = \frac{1}{k_1}\left(\frac{k_1}{M^{2(1-\beta)}k_2}\right)^{\frac{1-\alpha}{\beta-\alpha}}\left(\frac{1}{\beta-1} + \frac{1}{1-\alpha}\right),$$

where $k_1 = \min\{k_{11}, k_{12}\} = \min\{11, 10\} = 10,\ M = 2$

and $k_2 = \min\{k_{21}, k_{22}\} = \min\{6, 9\} = 6$ then $T_2 = 2.0617$.

From this, it is observed that the drive and response systems (32) and (33) are synchronized with each other, and the corresponding error with controller (34) is depicted through Figs. 7 and 8, and it is observed from the error graphs that systems reach their desired target within finite time.

Example 3. In order to demonstrate the application of the OVNNs, let us consider a 12×12 pixel color image pattern "F" illustrated in Fig. 9, and corresponding OVNNs given in (35) to store this image accurately. We have successfully constructed OVNNs consisting of 72 neurons, resulting in a 72-dimensional equilibrium point capable of storing the color

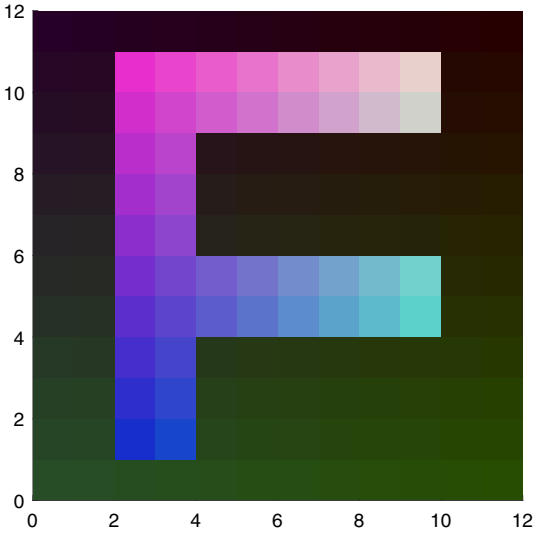

Fig. 9. Plot of the original color image of pattern "F".

image pattern "F." Let us take the OVNNs and their parameters as the following

$$\dot{x}_r(t) = -a_r x_r(t) + \Sigma_{j=1}^{M} b_{rj} f_j(x_j(t)) + \Sigma_{j=1}^{M} c_{rj} g_j(x_j(t - \tau_{rj}(t))) + \Sigma_{j=1}^{M} d_{rj} \int_{t-\sigma_{rj}(t)}^{t} h_j(x_j(s))ds + I_r, \tag{35}$$

where I_r is the external input. Assume that the parameters of the OVNNs (35) are defined as follows:

$$a_r = 1, \tag{36}$$

$$b_{rj} = \begin{cases} 4.0w_0 + 0.40w_1 - 0.30w_2 + 0.50w_3 + 0.40w_4 - 0.50w_5 \\ +0.50w_6 - 0.30w_7, & \text{if } r = j \\ 0.40w_0 - 0.50w_1 + 0.50w_2 - 0.30w_3 + 0.40w_4 - 0.50w_5 \\ +0.50w_6 - 0.30w_7, & \text{if } r \neq j \end{cases} \tag{37}$$

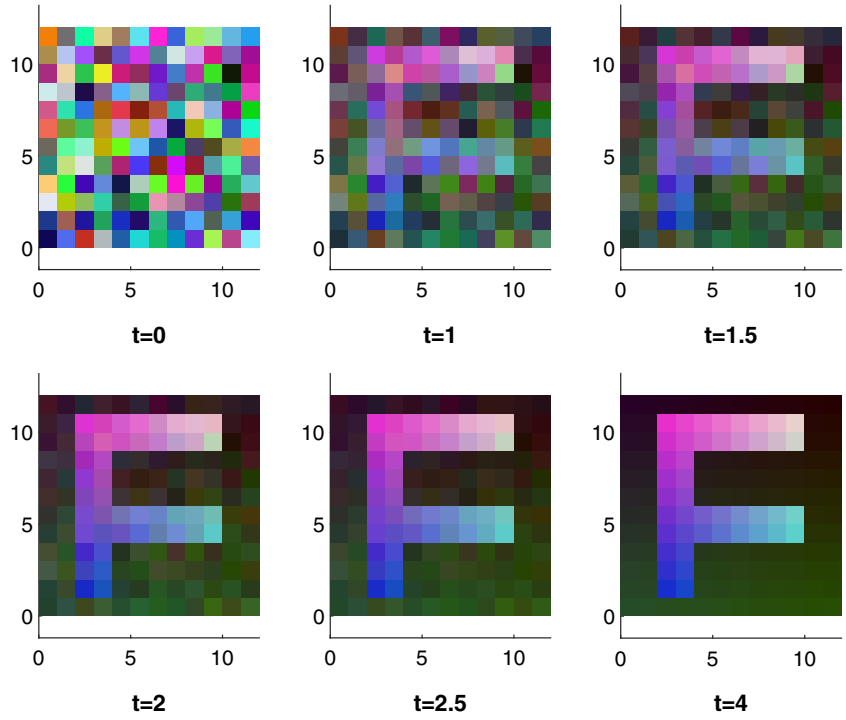

Fig. 10. Plots of numerical simulation for retrieving image pattern "F" with random initial values at time, $t = 0, 1, 1.5, 2, 2.5, 4$.

$$c_{rj} = \begin{cases} -0.20w_0 + 0.20w_1 - 0.50w_2 + 0.40w_3 - 0.20w_4 + 0.20w_5 \\ -0.50w_6 + 0.40w_7, & \text{if } r < j \\ 2.0w_0 + 0.30w_1 - 0.20w_2 - 0.30w_3 + 0.20w_4 + 0.20w_5 \\ -0.50w_6 + 0.40w_7, & \text{if } r = j \\ -0.10w_0 - 0.20w_1 + 0.30w_2 - 0.50w_3 + 0.10w_4 + 0.20w_5 \\ +0.30w_6 - 0.50w_7, & \text{if } r > j \end{cases} \tag{38}$$

$$d_{rj} = 0, \tag{39}$$

$$f_r^b(z) = g_r^b(z) = h_r^b(z) = \tanh(z^b(t)), \qquad \tau_{rj}(t) = 1, \tag{40}$$

for all $r, j = 1, 2, \ldots, 72$ and $b = 0, 1, \ldots, 7$. The equilibrium point of the proposed OVNNs must be $\mathbf{x} = (x_1, x_2, \ldots, x_{72}) \in \mathbf{O}^{72}$ to recall the image pattern "F", where

$$\begin{aligned} x_1 &= 0w_0 + 0.15w_1 + 0.3w_2 + 0.08w_3 + 0w_4 + 0.09w_5 + 0.45w_6 + 0.2w_7, \\ x_2 &= 0w_0 + 0.18w_1 + 0.45w_2 + 0.2w_3 + 0w_4 + 0.27w_5 + 0.45w_6 + 0.2w_7, \\ &\vdots \\ x_{71} &= 0w_0 + 0.55w_1 + 0.27w_2 + 0.2w_3 + 0w_4 + 0.64w_5 + 0.27w_6 + 0.2w_7, \\ x_{72} &= 0w_0 + 0.91w_1 + 0.73w_2 + 0.2w_3 + 0w_4 + 0.15w_5 + 0w_6 + 0.04w_7, \end{aligned}$$

which corresponds to the color {(0.27, 0.36, 0.2) and (0.09, 0.45, 0.2)}, {(0.18, 0.45, 0.2) and (0.15, 0, 0)}, {(0.55, 0.27, 0.2) and (0.64, 0.27, 0.2)} and {(0.91, 0.73, 0.2) and (0.15, 0, 0)} etc of pixels of pattern "F". Fig. 10 shows a simulation with random initial values. Now for above x the external input I is calculated as $\mathbf{I} = (I_1, I_2, \ldots, I_{72}) \in \mathbf{O}^{72}$, where the first few entries are:

$$\begin{aligned} I_1 &= -45.8w_0 + 35.95w_1 - 100.3w_2 + 87.55w_3 - 47w_4 - 230.9w_5 \\ &\quad + 2.82w_6 + 89.95w_7, \\ I_2 &= -47w_0 + 35.95w_1 - 109.9w_2 + 98.27w_3 - 48.2w_4 - 252.5w_5 \\ &\quad + 12.75w_6 + 98.4w_7, \\ &\vdots \\ I_{71} &= -39.8w_0 + 35.95w_1 - 52.46w_2 + 33.47w_3 - 41w_4 - 122.9w_5 \\ &\quad - 45.29w_6 + 47.87w_7, \\ I_{72} &= -35w_0 + 35.95w_1 - 14.17w_2 - 9.73w_3 - 36.2w_4 - 36.45w_5 \\ &\quad - 83.8w_6 + 14.27w_7. \end{aligned}$$

Due to space constraints, we only provide partial values for $\mathbf{x}$ and $\mathbf{I}$. The simulation results (see Fig. 10) with randomly selected initial conditions indicate that the proposed OVNNs, using parameters (36)–(40), successfully retrieve the true color image pattern "F."

Remark 16. Compared to existing results for storing true-color images, the OVNNs framework significantly reduces the number of required neurons. For example, the CVNN-based approach in [68] uses 432 neurons to store a 12×12 image, while the QVNN-based model in [48] reduces this to 144 neurons. In contrast, the proposed OVNNs architecture in Example 3 performs the same task with only 72 neurons, representing a reduction of 50 %. Although the authors of the article [62] have suggested that the storage capacity of OVNNs is larger compared to QVNNs and CVNNs, it is important to note that storing a 12×12 pixel color image requires 432 neurons in CVNNs, which is significantly higher. However, this article focuses specifically on OVNNs using the activation function tanh. Remarkably, the image "F" reconstruction is successfully approximated in a short time span of $t = 2.5$, demonstrating the fast convergence and practical effectiveness of the proposed OVNN framework.

5. Conclusion

This study examines the FTS and FTPS of OVNNs with mixed time delays. The investigation employs the one-norm and Lyapunov functions without using a separation technique. An inequality approach is utilized to analyze the results, supported by various norm properties established in Lemma 2 for the octonion domain. By transforming the one-norm, two effective controllers and several sufficient criteria have been introduced in the form of theorems to ensure FTS and FTPS in OVNNs and to estimate the corresponding settling time. Two numerical

examples have been considered to show the correctness of the numerical results of the proposed scheme with the simulation results, which have validated the effectiveness and efficiency of the proposed method. Finally, we present a practical example that highlights the advantages of OVNNs over neural networks with lower-dimensional architectures. This example clearly demonstrates how OVNNs, with their higher-dimensional structure, offer superior performance in handling complex data representations compared to networks with low dimensions.

Moreover, the gaps between the estimated settling time and the actual synchronization time have been acknowledged graphically. Our future research will aim to enhance the accuracy of settling time predictions for impulsive neural network systems with unbounded time delay factors. There are plans to develop these results further in the near future to establish preassigned time synchronization criteria for complex neural networks based on the one-norm approach. Furthermore, based on the one-norm approach and by generalizing Lemma 2, the proposed results can be extended to n-dimensional hypercomplex neural network systems, which represent the most general cases of complex, quaternion, and octonion-valued models for neural networks. Our next objective is to extend the application of FTS and FTPS to the octonion domain to rigorously demonstrate the effectiveness and applicability of fixed-time stability theory within the framework of octonion-valued neural networks.

CRediT authorship contribution statement

Vaibhav Agrawal: Writing – original draft, Methodology, Formal analysis, Conceptualization. **Sunny Singh:** Writing – original draft, Software, Validation, Methodology, Investigation, Formal analysis, Conceptualization. **Vineet Kumar Singh:** Validation, Investigation, Formal analysis, Conceptualization. **Subir Das:** Writing – review & editing, Visualization, Supervision.

Declaration of competing interest

The authors declare that they have no known competing financial interests or personal relationships that could have appeared to influence the work reported in this paper.

Acknowledgment

The authors express their sincere gratitude to the respected reviewers and editor for their valuable suggestions and constructive feedback, which have significantly contributed to the enhancement of this article's work.

Appendix A. Supplementary data

Supplementary data to this article can be found online at doi:10.1016/j.neucom.2025.130995.

Data availability

No external datasets were used in the research described in this article. All simulations and analyses were performed using self-developed models. The associated code and implementation details are part of ongoing work and may be made available upon reasonable request after publication.

References

[1] B. Yegnanarayana, Artificial Neural Networks, PHI Learning Pvt. Ltd., 2009.
[2] J. Zou, Y. Han, S.-S. So, Overview of artificial neural networks, Artif. Neural Netw.: Methods Appl. (2009) 14–22.
[3] S. Singh, U. Kumar, S. Das, J. Cao, Global exponential stability of inertial cohen–grossberg neural networks with time-varying delays via feedback and adaptive control schemes: non-reduction order approach, Neural. Process. Lett. 55 (4) (2023) 4347–4363.
[4] N. Zhao, Y. Qiao, J. Miao, L. Duan, New predefined-time stability results of impulsive systems with time-varying impulse strength and its application to synchronization of delayed BAM neural networks, Commun. Nonlinear Sci. Numer. Simul. 129 (2024) 107724.
[5] Q. Cui, L. Li, L. Wang, Exponential stability of delayed nonlinear systems with state-dependent delayed impulses and its application in delayed neural networks, Commun. Nonlinear Sci. Numer. Simul. 125 (2023) 107375.
[6] X. Liu, H. He, J. Cao, Event-triggered bipartite synchronization of delayed inertial memristive neural networks with unknown disturbances, IEEE Trans. Control Netw. Syst. 11 (3) (2023) 1408–1419.
[7] Q. Cui, C. Xu, Y. Xu, W. Ou, Y. Pang, Z. Liu, J. Shen, M.Z. Baber, C. Maharajan, U. Ghosh, Bifurcation and controller design of 5D BAM neural networks with time delay, Int. J. Numer. Model.: Electron. Netw. Devices Fields 37 (6) (2024) e3316.
[8] V.K. Shukla, M.C. Joshi, P.K. Mishra, C. Xu, Mechanical analysis and function matrix projective synchronization of el-nino chaotic system, Phys. Scr. 100 (1) (2024) 015255.
[9] V.K. Shukla, M.C. Joshi, P.K. Mishra, C. Xu, Adaptive fixed-time difference synchronization for different classes of chaotic dynamical systems, Phys. Scr. 99 (9) (2024) 095264.
[10] C. Xu, J. Lin, Y. Zhao, Q. Cui, W. Ou, Y. Pang, Z. Liu, M. Liao, P. Li, New results on bifurcation for fractional-order octonion-valued neural networks involving delays, Network: Comput. Neural Syst. (2024) 1–53, https://doi.org/10.1080/0954898X.2024.2332662.
[11] C. Xu, Z. Liu, L. Yao, C. Aouiti, Further exploration on bifurcation of fractional-order six-neuron bi-directional associative memory neural networks with multi-delays, Appl. Math. Comput. 410 (2021) 126458.
[12] B. Widrow, J. McCool, M. Ball, The complex LMS algorithm, Proc. IEEE 63 (4) (1975) 719–720.
[13] A. Hirose, Complex-Valued Neural Networks, vol. 400, Springer Science & Business Media, 2012.
[14] A. Hirose, Complex-Valued Neural Networks: Advances and Applications, vol. 18, Wiley-IEEE Press, 2013.
[15] C. Maharajan, C. Sowmiya, C. Xu, Delay dependent complex-valued bidirectional with stochastic and impulsive effects: an exponential stability approach, KYBERNETIKA 60 (3) (2024) 317–356.
[16] W.R. Hamilton, Lectures on Quaternions: Containing a Systematic Statement of a New Mathematical Method, Hodges and Smith, Dublin, 1853.
[17] B.C. Ujang, C.C. Took, D.P. Mandic, Quaternion-valued nonlinear adaptive filtering, IEEE Trans. Neural Netw. 22 (8) (2011) 1193–1206.
[18] C. Zou, K.I. Kou, Y. Wang, Quaternion collaborative and sparse representation with application to color face recognition, IEEE Trans. Image Process. 25 (7) (2016) 3287–3302.
[19] T. Isokawa, T. Kusakabe, N. Matsui, F. Peper, Quaternion neural network and its application, in: Knowledge-Based Intelligent Information and Engineering Systems: 7th International Conference, KES 2003, Oxford, UK, September 2003. Proceedings, Part II 7, vol. 2774, Springer, 2003, pp. 318–324.
[20] S. Singh, S. Das, J. Cao, Global dissipativity for quaternion valued inertial neural networks with unbounded time-varying delays, Math. Methods Appl. Sci. 48 (11) (2025) 10991–11006.
[21] S.L. Adler, Quaternionic Quantum Mechanics and Quantum Fields, vol. 88, Oxford University Press, 1995.
[22] T. Isokawa, N. Matsui, H. Nishimura, Quaternionic neural networks: fundamental properties and applications, in: Complex-Valued Neural Networks: Utilizing High-Dimensional Parameters, IGI global, 2009, pp. 411–439.
[23] S. Singh, S. Das, S.S. Chouhan, J. Cao, Anti-synchronization of inertial neural networks with quaternion-valued and unbounded delays: non-reduction and non-separation approach, Know. Based Syst. 278 (2023) 110903.
[24] S. Singh, U. Kumar, S. Das, F. Alsaadi, J. Cao, Synchronization of quaternion valued neural networks with mixed time delays using lyapunov function method, Neural. Process. Lett. 54 (2) (2022) 785–801.
[25] R. Wei, J. Cao, M. Abdel-Aty, Fixed-time synchronization of second-order mnns in quaternion field, IEEE Trans. Syst. Man Cybern.: Syst. 51 (6) (2019) 3587–3598.
[26] G. Chen, Y. Wang, X. Zhang, New global exponential synchronization conditions for impulsive chaotic neural networks with multiple time-varying leakage and transmission delays: applications for secure communications, Chaos Solitons Fract. 191 (2025) 115842.
[27] C.-A. Popa, Octonion-valued neural networks, in: Artificial Neural Networks and Machine Learning–ICANN 2016: 25th International Conference on Artificial Neural Networks, Barcelona, Spain, September 6-9, 2016, Proceedings, Part I 25, Springer, 2016.
[28] S.S. Chouhan, S. Das, J. Cao, et al Fixed time synchronization of octonion valued neural networks with time varying delays, Eng. Appl. Artif. Intel. 118 (2023) 105684.
[29] J. Xiao, X. Guo, Y. Li, S. Wen, K. Shi, Y. Tang, Extended analysis on the global mittag-leffler synchronization problem for fractional-order octonion-valued BAM neural networks, Neural Netw. 154 (2022) 491–507.
[30] X. Huang, Y. Li, Weyl almost periodic solutions of octonion-valued high-order fuzzy neural networks with delays, Comput. Appl. Math. 42 (4) (2023) 155.
[31] B. Li, Y. Cao, Y. Li, Almost periodic oscillation in distribution for octonion-valued neutral-type stochastic recurrent neural networks with d operator, Nonlinear Dyn. 111 (2023) 11371–11388.
[32] J. Wang, X. Liu. Global μ-stability and finite-time control of octonion-valued neural networks with unbounded delays, arXiv preprint arXiv:2003.11330, 2020.
[33] P. Kowsalya, S.S. Mohanrasu, A. Kashkynbayev, P. Gokul, R. Rakkiyappan, Fixed-time synchronization of inertial Cohen–Grossberg neural networks with state dependent delayed impulse control and its application to multi-image encryption, Chaos Solitons Fract. 181 (2024) 114693.
[34] L. Zhou, H. Lin, F. Tan, Fixed/predefined-time synchronization of coupled memristor-based neural networks with stochastic disturbance, Chaos Solitons Fract. 173 (2023) 113643.

[35] N. Zhao, Y. Qiao, J. Miao, L. Duan, Fixed-time synchronization of impulsive octonion-valued fuzzy inertial neural networks via improving fixed-time stability, IEEE Trans. Fuzzy Syst. 32 (4) (2023).
[36] T. Yu, J. Cao, L. Rutkowski, Y.-P. Luo, Finite-time synchronization of complex-valued memristive-based neural networks via hybrid control, IEEE Trans. Neural Netw. Learn. Syst. 33 (8) (2021) 3938–3947.
[37] J.-J. Xiong, G.-B. Zhang, J.-X. Wang, T.-H. Yan, Improved sliding mode control for finite-time synchronization of nonidentical delayed recurrent neural networks, IEEE Trans. Neural Netw. Learn. Syst. 31 (6) (2019) 2209–2216.
[38] A. Polyakov, Nonlinear feedback design for fixed-time stabilization of linear control systems, IEEE Trans. Autom. Control 57 (8) (2011) 2106–2110.
[39] T. Peng, J. Qiu, J. Lu, Z. Tu, J. Cao, Finite-time and fixed-time synchronization of quaternion-valued neural networks with/without mixed delays: an improved one-norm method, IEEE Trans. Neural Netw. Learn. Syst. 33 (12) (2021) 7475–7487.
[40] Z. Zhang, X. Wei, S. Wang, C. Lin, J. Chen, Fixed-time pinning common synchronization and adaptive synchronization for delayed quaternion-valued neural networks, IEEE Trans. Neural Netw. Learn. Syst. 35 (2) (2022).
[41] S. Jia, C. Hu, L. Feng, T. Shi, H. Jiang, Fixed/preassigned-time synchronization of quaternion-valued bam neural networks: an event-based non-separation control method, Commun. Nonlinear Sci. Numer. Simul. 137 (2024) 108145.
[42] L. Suo, M. Fečkan, J. Wang, Controllability and observability for linear quaternion-valued impulsive differential equations, Commun. Nonlinear Sci. Numer. Simul. 124 (2023) 107276.
[43] X. Liu, L. Wang, J. Cao, Further results on fixed-time leader-following consensus of heterogeneous multiagent systems with external disturbances, IEEE Trans. Syst. Man Cybern.: Syst. 54 (1) (2023) 416–425.
[44] H. Yan, Y. Qiao, J. Miao, Z. Ren, L. Duan, Fixed-time synchronization of delayed bam neural networks via new fixed-time stability results and non-chattering quantized controls, J. Franklin Inst. 360 (13) (2023) 10251–10274.
[45] H. Yan, Y. Qiao, Z. Ren, L. Duan, J. Miao, A novel fixed-time stability result and its application to synchronization of delayed multidirectional associative memory neural networks with discontinuous activations, Neurocomputing 542 (2023) 126275.
[46] X. Qin, H. Jiang, J. Qiu, C. Hu, X. Li, Projective synchronization in fixed/predefined-time for quaternion-valued bam neural networks under event-triggered aperiodic intermittent control, Commun. Nonlinear Sci. Numer. Simul. 137 (2024) 108139.
[47] L. Liu, M. Lei, H. Bao, Event-triggered quantized quasisynchronization of uncertain quaternion-valued chaotic neural networks with time-varying delay for image encryption, IEEE Trans. Cybern. 53 (5) (2022) 3325–3336.
[48] Q. Song, X. Chen, Multistability analysis of quaternion-valued neural networks with time delays, IEEE Trans. Neural Netw. Learn. Syst. 29 (11) (2018) 5430–5440.
[49] C.-A. Popa, Global exponential stability of octonion-valued neural networks with leakage delay and mixed delays, Neural Netw. 105 (2018) 277–293.
[50] H. Deng, H. Bao, Fixed-time synchronization of quaternion-valued neural networks, Physica A Stat. Mech. Appl. 527 (2019) 121351.
[51] Z. Tu, Y. Zhao, N. Ding, Y. Feng, W. Zhang, Stability analysis of quaternion-valued neural networks with both discrete and distributed delays, Appl. Math. Comput. 343 (2019) 342–353.
[52] X. Song, J. Man, S. Song, C.K. Ahn, Finite/fixed-time anti-synchronization of inconsistent markovian quaternion-valued memristive neural networks with reaction-diffusion terms, IEEE Trans. Circuits Syst. I: Regul. Pap. 68 (1) (2020) 363–375.
[53] Z. Li, X. Liu, Finite time anti-synchronization of quaternion-valued neural networks with asynchronous time-varying delays, Neural. Process. Lett. 52 (3) (2020) 2253–2274.
[54] X. Liao, G. Chen, E.N. Sanchez, Delay-dependent exponential stability analysis of delayed neural networks: an LMI approach, Neural Netw. 15 (7) (2002) 855–866.
[55] S. Arik, Stability analysis of delayed neural networks, IEEE Trans. Circuits Syst. I 47 (7) (2000) 1089–1092.
[56] Z. Li, Y. Bai, C. Huang, H. Yan, S. Mu, Improved stability analysis for delayed neural networks, IEEE Trans. Neural Netw. Learn. Syst. 29 (9) (2017) 4535–4541.
[57] M. Forti, S. Manetti, M. Marini, Necessary and sufficient condition for absolute stability of neural networks, IEEE Trans. Circuits Syst. I 41 (7) (1994) 491–494.
[58] Z. Zhang, A. Li, S. Yu, Finite-time synchronization for delayed complex-valued neural networks via integrating inequality method, Neurocomputing 318 (2018) 248–260.
[59] R. Guo, J. Lu, Y. Li, W. Lv, Fixed-time synchronization of inertial complex-valued neural networks with time delays, Nonlinear Dyn. 105 (2021) 1643–1656.
[60] L. Mi, C. Chen, B. Qiu, L. Xu, L. Zhang, Fixed-time synchronization analysis for complex-valued neural networks via a new fixed-time stability theorem, IEEE Access 8 (2020) 172799–172807.
[61] U. Kumar, S. Das, C. Huang, J. Cao, Fixed-time synchronization of quaternion-valued neural networks with time-varying delay, Process. R. Socitey A 476 (2241) (2020) 20200324.
[62] S.S. Chouhan, R. Kumar, S. Sarkar, S. Das, Multistability analysis of octonion-valued neural networks with time-varying delays, Inf. Sci. (Ny) 609 (2022) 1412–1434.
[63] J. Wang, X. Liu, Finite time stability of octonion-valued neural networks with delays, in: 2021 36th Youth Academic Annual Conference of Chinese Association of Automation (YAC), IEEE, 2021, pp. 55–60.
[64] T. Peng, Y. Wu, Z. Tu, A.S. Alofi, J. Lu, Fixed-time and prescribed-time synchronization of quaternion-valued neural networks: a control strategy involving lyapunov functions, Neural Netw. 160 (2023) 108–121.
[65] V.K. Shukla, M.C. Joshi, P.K. Mishra, Y. Mousavi, M.R. Zadeh, A. Fekih, Predefined synchronization of mixed and leakage-delayed quaternion-valued neural network, Int. J. Dyn. Control. 13 (2) (2025) 51.
[66] X. Xu, J. Zhang, J. Shi, Exponential stability of complex-valued neural networks with mixed delays, Neurocomputing 128 (2014) 483–490.
[67] X. Lv, X. Li, Delay-dependent dissipativity of neural networks with mixed non-differentiable interval delays, Neurocomputing 267 (2017) 85–94.
[68] P. Zheng, Threshold complex-valued neural associative memory, IEEE Trans. Neural Netw. Learn. Syst. 25 (9) (2013) 1714–1718.

Author biography

Vaibhav Agrawal was born in Rajasthan, India, in 1998. He received his B.Sc. degree from the University of Rajasthan, Jaipur, India, in 2017, and his M.Sc. degree in Applied Mathematics from Jiwaji University, Gwalior, India, in 2019. He is currently pursuing a Ph.D. in the Department of Mathematical Sciences at the Indian Institute of Technology (BHU), Varanasi, India, as a University Grants Commission (UGC) fellow. Since 2022, he has been engaged in research on the nonlinear dynamics of neural networks under the supervision of Prof. Vineet Kumar Singh and Prof. Subir Das.

Dr. Sunny Singh was born in Uttar Pradesh, India, in 1992. He received his M.Sc. degree in Applied Mathematics from Deen Dayal Upadhyaya Gorakhpur University, Gorakhpur, India, in 2016, and his Ph.D. degree in Mathematics from the Indian Institute of Technology (Banaras Hindu University), Varanasi, India, in 2024. He is currently a Postdoctoral Researcher at TU Delft, Netherlands. Since 2019, his research has focused on nonlinear dynamics, control theory, neural networks and machine learning.

Prof. Vineet Kumar Singh received M.Sc. Degree in Applied Mathematics from Udai Pratap Autonomous College, Varanasi, India in 2003 and Ph.D. degree in Applied Mathematics from Indian Institute of Technology (Banaras Hindu University), Varanasi, India in 2009. He is currently a Professor with Department of Mathematical Sciences, IIT (BHU), Varanasi, India. He has supervised 12 scholars for their doctoral program. His current research interests include numerical analysis, computational methods for integral and differential Equations, fractional calculus, mathematical biology nonlinear dynamics.

Prof. Subir Das received his M.Sc. degree in Applied Mathematics from the University of Calcutta, India, and his Ph.D. degree in Applied Mathematics from the Indian Institute of Engineering Science and Technology (IIEST), Shibpur, India. He was awarded the Griffith Memorial Award by the University of Calcutta in 2001. He is currently a Professor in the Department of Mathematical Sciences at the Indian Institute of Technology (BHU), Varanasi, India. Prof. Das has supervised 37 Ph.D. scholars and 50 postgraduate students. To date, he has published 262 research articles in reputed international journals. His current research interests include fracture mechanics, mathematical modelling, porous media, and nonlinear dynamics.